Bioscience Reports (2022) **42** BSR20220800
https://doi.org/10.1042/BSR20220800

PORTLAND PRESS

Research Article

Gene expression profile associated with Asmt knockout-induced depression-like behaviors and exercise effects in mouse hypothalamus

Wenbin Liu[1,2,*], Zhuochun Huang[1,2], Jie Xia[1,2], Zhiming Cui[1,2], Lingxia Li[1,2], Zhengtang Qi[1,2] and Weina Liu[1,2,*]

[1]Key Laboratory of Adolescent Health Assessment and Exercise Intervention of Ministry of Education, East China Normal University, Shanghai 200241, China; [2]College of Physical Education and Health, East China Normal University, Shanghai 200241, China

Correspondence: Weina Liu (wnliu@tyxx.ecnu.edu.cn) or Zhengtang Qi (ztqi@tyxx.ecnu.edu.cn)

Sleep disorder caused by abnormal circadian rhythm is one of the main symptoms and risk factors of depression. As a known hormone regulating circadian rhythms, melatonin (MT) is also namely N-acetyl-5-methoxytryptamine. N-acetylserotonin methyltransferase (Asmt) is the key rate-limiting enzyme of MT synthesis and has been reportedly associated with depression. Although 50–90% of patients with depression have sleep disorders, there are no effective treatment ways in the clinic. Exercise can regulate circadian rhythm and play an important role in depression treatment. In the present study, we showed that Asmt knockout induced depression-like behaviors, which were ameliorated by swimming exercise. Moreover, swimming exercise increased serum levels of MT and 5-hydroxytryptamine (5-HT) in Asmt knockout mice. In addition, the microarray data identified 10 differentially expressed genes (DEGs) in KO mice compared with WT mice and 29 DEGs in KO mice after swimming exercise. Among the DEGs, the direction and magnitude of change in epidermal growth factor receptor pathway substrate 8-like 1 (Eps8l1) and phospholipase C-β 2 (Plcb2) were confirmed by qRT-PCR partly. Subsequent bioinformatic analysis showed that these DEGs were enriched significantly in the p53 signaling pathway, long-term depression and estrogen signaling pathway. In the protein–protein interaction (PPI) networks, membrane palmitoylated protein 1 (Mpp1) and p53-induced death domain protein 1 (Pidd1) were hub genes to participate in the pathological mechanisms of depression and exercise intervention. These findings may provide new targets for the treatment of depression.

Introduction

Sleep disorders caused by abnormal circadian rhythm have been widely demonstrated in patients with depression [1,2]. However, most of the current antidepressants have a weak therapeutic effect on sleep disorders [3], such as selective serotonin reuptake inhibitor (SSRI) and selective norepinephrine reuptake inhibitor (SNRI), which are based on the monoamine hypothesis [4]. 5-Hydroxytryptamine (5-HT), a kind of monoamine neurotransmitter, can be catalyzed by N-acetyl serotonin methyltransferase (Asmt) via N-acetyl serotonin to form melatonin (MT) [5]. Clinically, MT level decreases in patients with depression, and MT treatment can prolong sleep time and alleviate depression [6]. Animal studies have also confirmed the rapid and lasting anti-depression and anti-anxiety effects of MT in chronic stress rats [7]. Therefore, it is of great significance to explore the regulatory factors of MT secretion in depression.

In the pineal, arylalkylamine N-acetyltransferase (AANAT) and Asmt are both key rate-limiting enzymes affecting MT biosynthesis. Asmt plays a catalytic role in the last step of the synthesis reaction and has been found to be associated with depression [8]. The mRNA and protein expression levels of Asmt

*These authors contributed equally to this work.

Received: 15 April 2022
Revised: 16 June 2022
Accepted: 29 June 2022

Accepted Manuscript online: 30 June 2022
Version of Record published: 14 July 2022

Bioscience Reports (2022) **42** BSR20220800
https://doi.org/10.1042/BSR20220800

were significantly lower in patients with recurrent depression than those in healthy individuals [9]. It has been reported that single nucleotide polymorphism of Asmt gene is implicated in depression, the AA genotype at rs4446909 and GG genotype at rs5989681 in the promoter B region of Asmt gene were protective genes of depression [10]. Similarly, Asmt gene polymorphism has been reportedly relevant to the susceptibility of autism spectrum disorders [10] and bipolar disorders [11]. Therefore, the first aim of the present study is to identify whether Asmt knockout induces depression-like behaviors in mice, thus being employed as a useful model to study depression with sleep disorders.

Exercise has been found to regulate the phase of MT rhythm and the sleep–wake cycle [12], as well as circadian adaptation [13] by regulating MT level [14]. Moreover, exercise is an effective treatment for major depression [15]. Among the many challenges related to depression, lack of biomarkers for diagnosis appears especially prominent. Gene chip, also called DNA chip or DNA microarray, is an appropriate tool to address this issue [16]. In recent years, gene chip has been widely used in the research fields of depression [17], exercise [18], and exercise intervention for depression [19]. Therefore, the second aim of the current study is to investigate the effects of Asmt knockout and swimming exercise on gene expression profiles in mice, which may provide selective biomarkers for depression.

Materials and methods

Animals and groups

Mice were obtained from Humangen Biotech Inc. (Shanghai, China). Asmt-knockout mice (F0) were generated via co-injection of *in vitro*-synthesized Asmt sgRNA (5′-gCGCCTACACCAACTCCCCCC-3′), Cas9 mRNA and pMD19T-T7 vector into the zygotes of C57BL/6 mice [20]. Mouse Asmt gene (ID: 107626) is located in the F5 region of X chromosome, and a total of 5 SgRNAs were designed for exons 2 and 3, and the splicing efficiency was tested in NIH3T3 cells. The founder mice was analyzed with quantitative real-time polymerase chain reaction (qRT-PCR) using the set of primers (sense 5'-agggtcacagttcatggtgg-3' and antisense 5'-tcgacgcccacggccctcgcgta-3'). The initially obtained Asmt-knockout mice (i.e., the positive founder mice with 20 bp deletion, F0) from Humangen Biotech Inc. were backcrossed with their wild-type littermates C57BL/6 mice for three generations. Genotyping was conducted with high resolution melting (HRM) analysis after qRT-PCR, which can distinguish three genotypes accurately [21].

Mice were housed with a 12-h light:dark cycle under controlled temperature (22 $\pm$ 2°C) and humidity (50 $\pm$ 10%), and were given standard diet and water ad libitum. The breeding male mice (3- to 4-week old, 17–20 g) were performed gene identification to select Asmt-knockout homozygous mice and wild-type littermate mice. All mice were adaptively reared for 3 weeks, and were then trained in a swimming program or not. Mice were randomly assigned to four groups: wild-type control group (WT, n=5), Asmt-knockout control group (KO, n=5), wild-type exercise group (WE, n=4), and Asmt-knockout exercise group (KE, n=5). All animal work has taken place in the Experimental Animal Centre at East China Normal University, Shanghai, China.

Exercise protocol

As described in studies of ours [22] and others [23], WE and KE mice were trained in a moderate swimming process with no weight loading in free style. Daily swimming exercise was performed in a large glass water tank [100 cm (L) $\times$ 60 cm (W) $\times$ 80 cm (H)] at 32 $\pm$ 1°C. The exercise period began when mice were at the age of 6–7 weeks. During the first week for adaptation, the training was graded beginning with 10 min on the first day until 60 min on the last day. Thereafter, regular training period began with intensity of 60 min/day, 6 d/week for 4 weeks. Exercise was performed at the same time every day (between 9:00 and 11:00 a.m.).

Behavioral testing

Except sucrose preference, a videocomputerized tracking system (DigBehav, Jiliang Co. Ltd., Shanghai, China) was used to record the behavioral changes of the animals. These behavioral tests were performed as described in our previous study [24].

Sucrose preference test (SPT)

In the SPT, sweetness preference decreases in depressed mice [25]. Briefly, 72 h before the test mice were trained to adapt 1% sucrose solution (w/v): two bottles of 1% sucrose solution were placed in each cage, and 24 h later 1% sucrose in one bottle was replaced with tap water for 24 h. After adaptation, mice were deprived of water and food for 24 h. Thereafter, mice housed in individual cages had free access to two bottles respectively containing 200 ml of sucrose solution (1% w/v) and 200 ml of water. At the end of 24 h, the sucrose preference was calculated as a percentage of the consumed 1% sucrose solution relative to the total amount of liquid intake.

Forced swim test (FST)

The FST is one of the most used tools for screening antidepressants among all animal models [26]. The swimming sessions were conducted by placing the mice in cylinders (30 cm height × 10 cm diameters) containing 25°C water 20 cm deep so that the mice could not support themselves by touching the bottom with their feet. The FST was conducted for 5 min, during which immobility time and struggling time was recorded. Floating in the water without struggling and only making movements necessary to keep its head above the water were regarded as immobility.

Open field test (OFT)

The OFT is employed to evaluate the effects of antidepressant treatment [27]. Each mouse was placed in the center of the open field (30 × 30 × 30 cm chamber, with 16 holes in its floor, each hole had infrared sensing) for 5 min in a quiet room. The parameter assessed was the number of poking into holes.

Sample collection

Mice were decapitated after isoflurane anesthesia and blood was kept in room temperature, and then was centrifuged at 3000 rpm for 10min to separate the serum and blood cells. The hypothalamus was rapidly and carefully separated on ice-plate, in view of regulating effects of hypothalamus on sleep, mood, circadian, and seasonal rhythm [28]. The serum and hypothalamus were stored at −80°C until assays.

Enzyme-linked immunosorbent assay (ELISA)

Serum concentrations of MT and 5-HT were determined using commercially ELISA kits (Shanghai Enzyme-linked Biotechnology Co., Ltd., Shanghai, China) following the manufacturer's instructions.

Agilent transcriptome microarray assay

The collected hypothalamus tissues were put into dry ice and sent to OE Biotech Co., Ltd (Shanghai, China) for the One-Color Microarray-Based Gene Expression Detection and Analysis. Each group included three samples. The gene expression profiles were conducted using Agilent SurePrint G3 Mouse Gene Expression V2.0 (8 × 60K, Design ID: 074809).

Expression profile microarray experiments

Total RNA was quantified by NanoDrop ND-2000 (Thermo Scientific) and the RNA integrity was assessed using Agilent Bioanalyzer 2100 (Agilent Technologies). The RNA integrity assessment results of all samples were very good, with A (RNA Integrity Number [RIN] $\geq$7 and 28S/18S $\geq$ 0.7), which means these samples can be used in subsequent experiments. The sample labeling, microarray hybridization, and washing were performed according to the manufacturer's standard protocols. After washing, the arrays were scanned by Agilent Scanner G2505C (Agilent Technologies) to get the array images. The raw data were extracted from the images by Feature Extraction software (version10.7.1.1, Agilent Technologies) finally.

Differentially expressed genes identification

Genespring (version 13.1, Agilent Technologies) was employed to process the basic analysis with the raw data. To begin with, the raw data were normalized with the quantile algorithm. The probes that at least 100% of the values in any 1 out of all conditions have flags in "Detected" were chosen for further data analysis. Differentially expressed genes (DEGs) were then identified through fold change as well as P value calculated with unpaired t-test. The screening criterion of DEGs was that the absolute fold change (FC-abs) $\geq$ 2.0 and $P \leq 0.05$. Afterward, Hierarchical Clustering (shown in the heatmap) was performed to display the differential gene expression pattern among samples by MeV 4.6 software, and the parameters were "Distance Metrics, Euclidean Distance, Linkage Method, Complete linkage".

Bioinformatics analysis of expression profiles

Briefly, function annotations including biological process (BP), cellular component (CC), and molecular function (MF) were obtained based on the Gene Ontology (GO) project (http://geneontology.org/). And enriched pathways were identified using the Kyoto Encyclopedia of Genes and Genomes (KEGG) project (http://www.genome.jp/kegg/). The GO and KEGG terms were pondered significant if $P<0.05$ or 0.1.

To locate potential therapeutic targets among identified DEGs, the protein–protein interaction (PPI) networks were constructed by Search Tool for Retrieval of Interacting Genes/Proteins (STRING, version 9.0, https://string-db.org/) and Cytoscape software (version 3.2.1, http://cytoscape.org/). The minimum required interaction score was set as

Bioscience Reports (2022) **42** BSR20220800
https://doi.org/10.1042/BSR20220800

0.15 in the STRING online database. Cytoscape software was used to visualize the PPI network, and the CytoHubba plugin for Cytoscape was used to calculate the degree value to screen the hub genes.

qRT-PCR validation

The hypothalamus tissues were performed by qRT-PCR to exclude false-positive results and validate microarray assay results further. Total RNA was extracted from frozen tissues using TRIzol (Invitrogen, Chromos, Singapore) and purified according to the instructions included. Then, double-stranded cDNA was synthesized from ∼1 μg of total RNA using ReverTra Ace® qPCR RT Kit (TOYOBO, Osaka, Japan). Real-time PCR kit (TOYOBO, Osaka, Japan) was used to prepare the 20 μl reaction system, including 4 pmol of each primer, 2.0× Master SYBR Green I (contains Taq DNA polymerase, reaction buffer, dNTP mix, SYBR Green I dye, and 10 mM $MgCl_2$), and 2.0 μl template. Real-time PCR reactions were cycled in QuantStudio 3 Real-Time PCR Instrument (Applied Biosystems, CA, U.S.A.). The amplification occurred in a three-step cycle (denaturation at 95°C for 15 s, annealing at 61°C for 30 s, extension and data collection at 72°C for 45 s) for 40 cycles. The target gene expression was normalized to internal standard 18S. Fold changes in the expression of genes of interest were calculated using the $2^{-\Delta\Delta Ct}$ method. According to mouse EST sequences of epidermal growth factor receptor pathway substrate 8-like 1 (Eps8l1), phospholipase C-β2 (Plcb2), synaptotagmin-like 2 (Sytl2), checkpoint kinase 1 (Chek1), cyclin-dependent kinase inhibitor 1A (Cdkn1a), inositol 1,4,5-triphosphate receptor 2 (Itpr2), transformed mouse 3T3 cell double minute 4 (Mdm4), p53 induced death domain protein 1 (Pidd1), heat shock protein family A member 1B (Hspa1b) and 18S in NCBI database. Primer Premier 3.0 software was used to design the primers. Primer sets used in the present study were shown in Supplementary Table S1.

Statistical analysis

Data are presented as mean ± SEM. Analyses were performed using GraphPad Prism Software (version 6.01). The statistical significance of differences was determined using two-way ANOVA followed by Bonferroni test for post hoc comparisons. Statistical significance was set at $P<0.05$ or 0.1.

Results

Effects of Asmt knockout and swimming exercise on depression-like behaviors and serum levels of MT and 5-HT

First, we demonstrated that Asmt knockout induced depression-like behaviors, including reduced percentage of sucrose preference in SPT ($P<0.01$, Figure 1A) and poking number in OFT ($P<0.01$, Figure 1D), compared with WT group. Swimming exercise ameliorated depression-like behaviors induced by Asmt knockout, including increased percentage of sucrose preference in SPT ($P<0.01$, Figure 1A), struggling time in FST ($P<0.05$, Figure 1C) and poking number in OFT ($P<0.01$, Figure 1D), as well as decreased immobility time in FST ($P<0.05$, Figure 1B). No KO × swim interaction on behavioral testing was found.

Then, we examined the serum levels of MT and 5-HT in hypothalamus. No main effects of Asmt knockout were found on the levels of MT or 5-HT, whereas swimming exercise increased the levels of MT ($P<0.05$, Figure 1E) and 5-HT ($P<0.01$, Figure 1F). A significant KO × swim interaction was found on MT level ($F_{(1, 11)} = 4.853$, $P<0.05$), suggesting the association among MT, Asmt, and swim.

Identification of DEGs after Asmt knockout and swimming exercise

According to the strict screening criteria mentioned above, we identified a large number of DEGs, the overall results were presented in Supplementary Table S2. Of these DEGs, 7 up-regulated and 3 down-regulated genes were identified in mice hypothalamus following Asmt knockout, compared with WT group (Figure 2A and Supplementary Table 3). In addition, 17 up-regulated and 12 down-regulated genes were identified in mice hypothalamus after swimming exercise, compared to KO group (Figure 2B and Supplementary Table S4). The top 10 up-regulated and down-regulated DEGs of the other comparisons among groups were shown in Figure 2C–E, and details were listed in Supplementary Tables S5–7.

Validation of DEGs by qRT-PCR

To validate the microarray results, we selected nine DEGs based on *P*-value and FC-abs, the mean of expression quantity and association with Asmt or exercise, and then performed qRT-PCR. These nine DEGs included Eps8l1, Plcb2, Sytl2, Chek1, Cdkn1a, Itpr2, Mdm4, Pidd1, and Hspa1b. The qRT-PCR results of Eps8l1 (Figure 3A) and

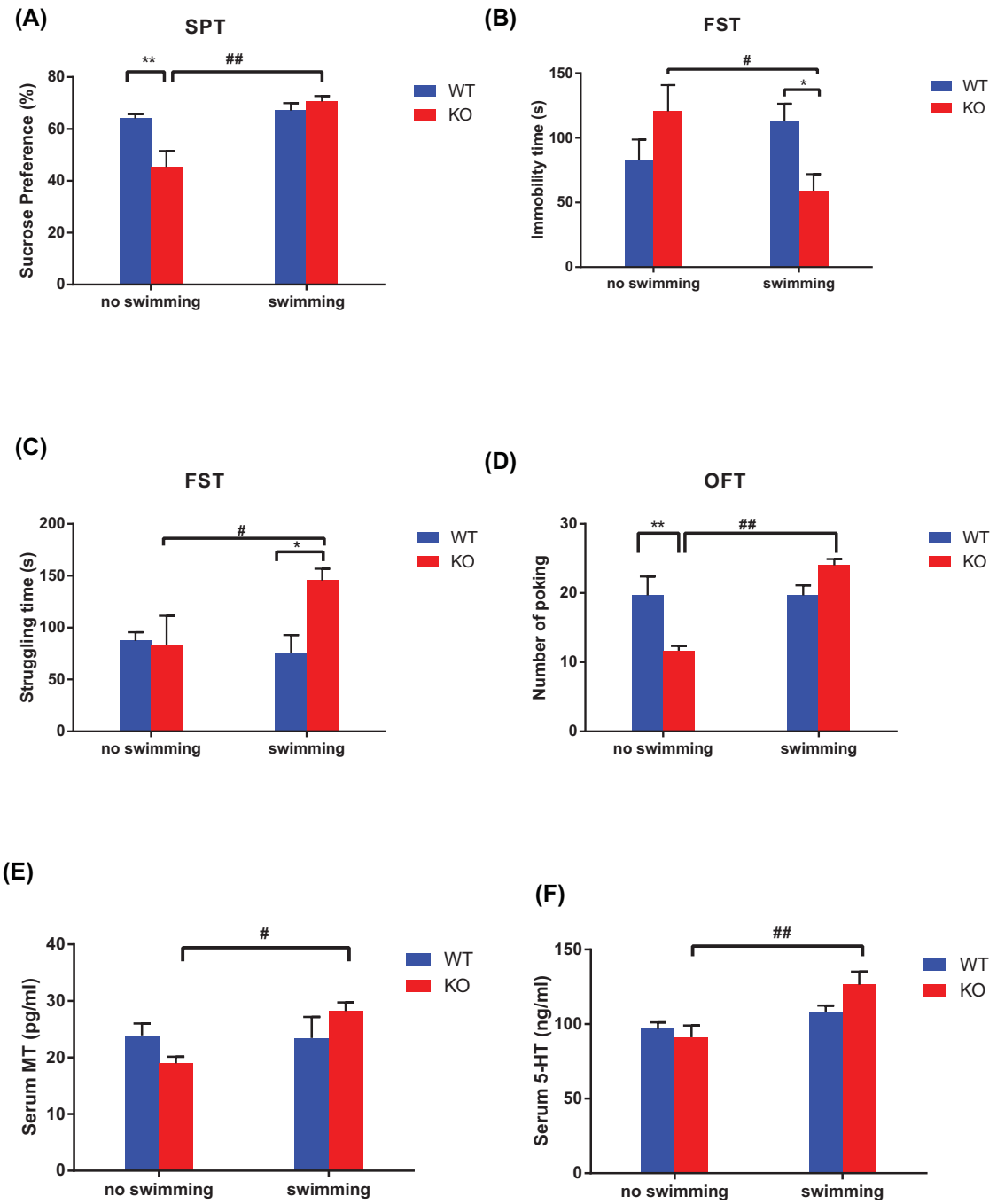

Figure 1. Effects of Asmt knockout and swimming exercise on depression-like behaviors and serum hormone levels in mice

(**A–D**) Depression-like behaviors: (A) Sucrose preference in sucrose preference test (SPT); (B) Immobility time in forced swim test (FST); (C) Struggling time in FST, (D) Poking number in open field test (OFT); (**E** and **F**) Serum hormone levels: (E) melatonin (MT), (F) 5-hydroxytryptamine (5-HT). Data are presented as means ± SEM ($n = 3$–5 per group). *$P<0.05$, **$P<0.01$ versus WT; #$P<0.05$, ##$P<0.01$ versus no swimming.

Bioscience Reports (2022) **42** BSR20220800
https://doi.org/10.1042/BSR20220800

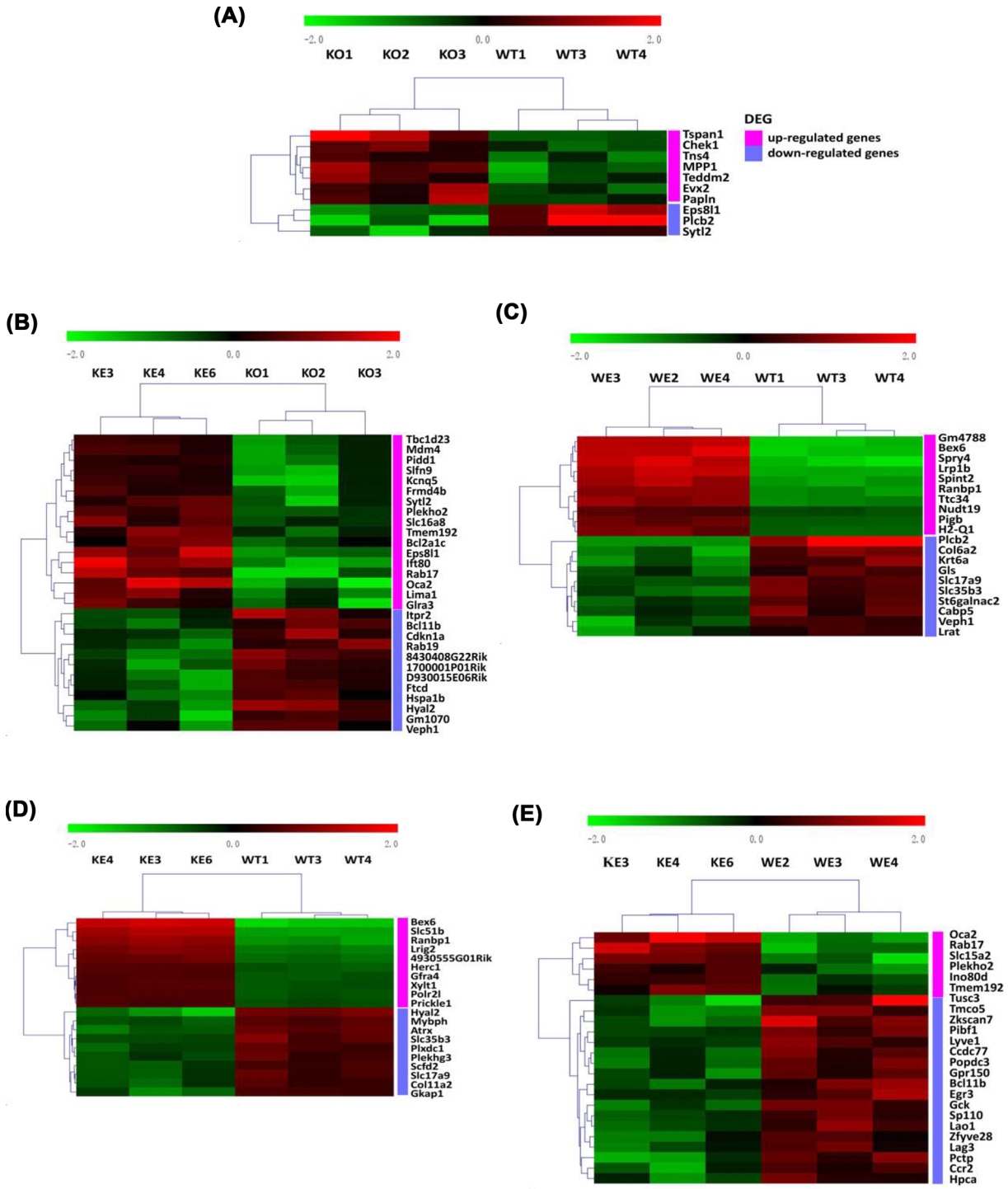

Figure 2. Heatmaps of the DEGs in mice hypothalamus

(**A**) Asmt-knockout control group (KO) versus wild-type control group (WT), (**B**) Asmt-knockout exercise group (KE) versus KO, (**C**) wild-type exercise group (WE) versus WT, (**D**) KE versus WT, (**E**) KE versus WE. Color scale represents gene expression value from relatively low (green) to relatively high (red).

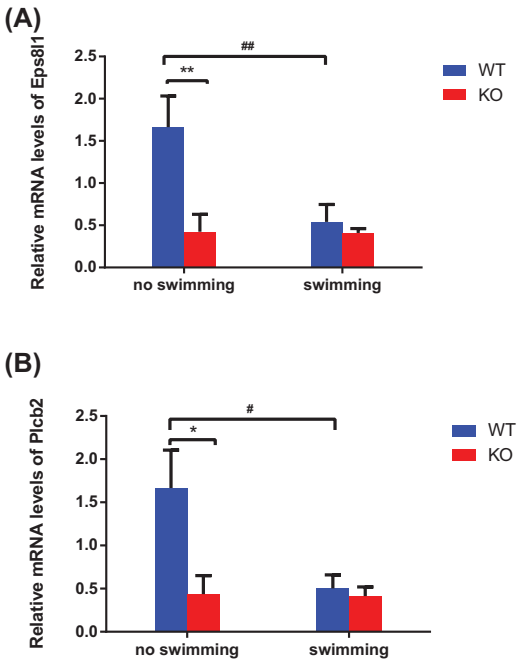

Figure 3. Validation of DEGs by qRT-PCR

The expression levels of epidermal growth factor receptor pathway substrate 8-like 1 (Eps8l1, **A**) and phospholipase C-β 2 (Plcb2, **B**) in mice hypothalamus with response to Asmt knockout and swimming exercise. The relative mRNA levels were conducted using qRT-PCR. Data are presented as means ± SEM ($n = 3$ per group). *$P<0.05$, **$P<0.01$ versus WT; #$P<0.05$, ##$P<0.01$ versus no swimming.

Plcb2 (Figure 3B) were consistent with the microarray data. The mRNA levels of Eps8l1 and Plcb2 were significantly down-regulated following Asmt knockout in mice, verifying the reliability of hypothalamus gene expression profiles. In view of enriched functions of Eps8l1 (Supplementary Table S8) and Plcb2 (Supplementary Table S9), we can infer that Eps8l1 and Plcb2 were related to Asmt knockout-induced depression-like behaviors. In addition, it needs to be further proved whether Eps8l1 and Plcb2 are involved in antidepressant effects of swimming exercise. The validation results of the other seven genes were shown in Supplementary Figure S1.

Enrichment analysis of DEGs after Asmt knockout and swimming exercise

The function enrichment analysis of DEGs was conducted by GO analysis. Following Asmt knockout in mice, the most prominent terms of BP, CC and MF were respectively involved in "sensory perception of bitter taste" (P=0.003288), "exocytic vesicle" (P=0.005665) and "phospholipase C activity" (P=0.004805); Figure 4A and Supplementary Table S10. After swimming exercise in KO mice, the most prominent terms of BP, CC, and MF were respectively involved in "cellular response to UV-B" (P=8.09E-05), "melanosome" (P=0.000636) and "extracellular-glycine -gated chloride channel activity" (P=0.007847); Figure 4B and Supplementary Table S11. The top 10 enriched GO terms generated by the other comparisons among groups were presented in Figure 4C–E, and details were listed in Supplementary Tables S12–14.

The pathway enrichment analysis of DEGs was further conducted to gain deeper insight into the effects of Asmt knockout and swimming exercise on depression-like behaviors. Based on the KEGG database, three pathways were significantly enriched following Asmt knockout and swimming exercise, such as p53 signaling pathway, long-term depression (LTD), and estrogen signaling pathway, but the involved genes were different in each comparison (Figure 5A,B and Supplementary Tables 15–17). The top 20 enriched KEGG terms generated by the other comparisons among groups were presented in Figure 5C–E, and details were listed in Supplementary Tables 18–20.

Bioscience Reports (2022) **42** BSR20220800
https://doi.org/10.1042/BSR20220800

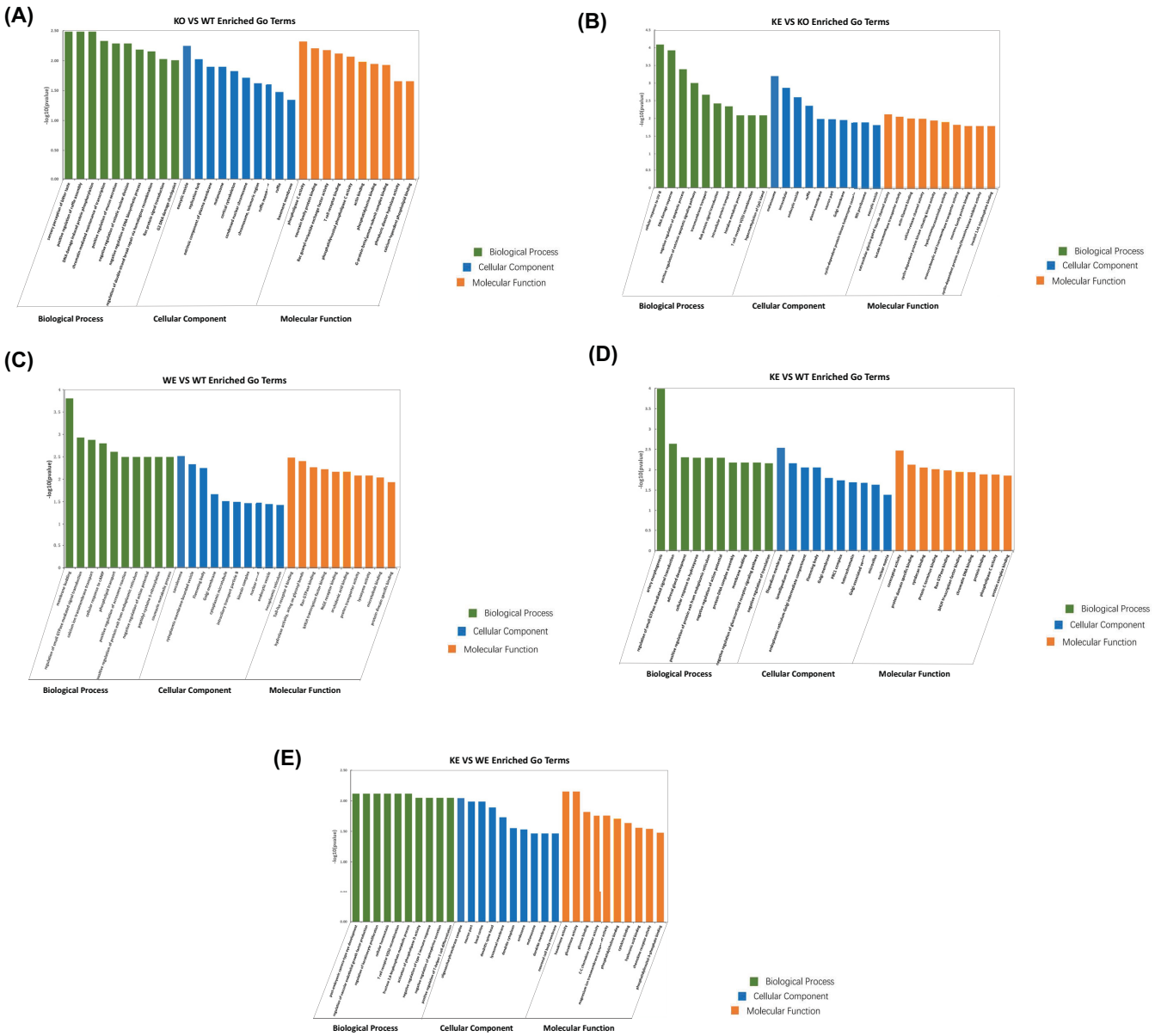

Figure 4

Figure 4. Gene Ontology (GO) analysis of DEGs

(**A**) KO versus WT, (**B**) KE versus KO, (**C**) WE versus WT, (**D**) KE versus WT, and (**E**) KE versus WE. Bar charts of function enrichment analysis were constructed by -log10 (*P* value) and the top 10 GO terms. The bar color represents GO terms related to Biological Process (green), Cellular Component (blue) and Molecular Function (orange).

PPI network construction of DEGs

Generally, a gene with a higher degree in the PPI networks is capable of causing more variation in regulation processes. A PPI network including 3 nodes and 2 edges was constructed (Figure 6A), up-regulated membrane palmitoylated protein 1 (Mpp1) (degree = 2) may be involved in the molecular mechanisms of Asmt knockout-induced depression-like behaviors. In addition, a PPI network including 15 nodes and 18 edges was constructed (Figure 6B), up-regulated Pidd1 (degree = 8) may be involved in the regulation mechanisms of swimming exercise for depression-like behaviors. The PPI networks of the other comparisons among groups were shown in Figure 6C–E.

In order to further investigate the roles of identified DEGs in the development of depression, then we constructed another network (Figure 6F) among Asmt, brain-derived neurotrophic factor (Bdnf), MT receptors (Mtnr1a and

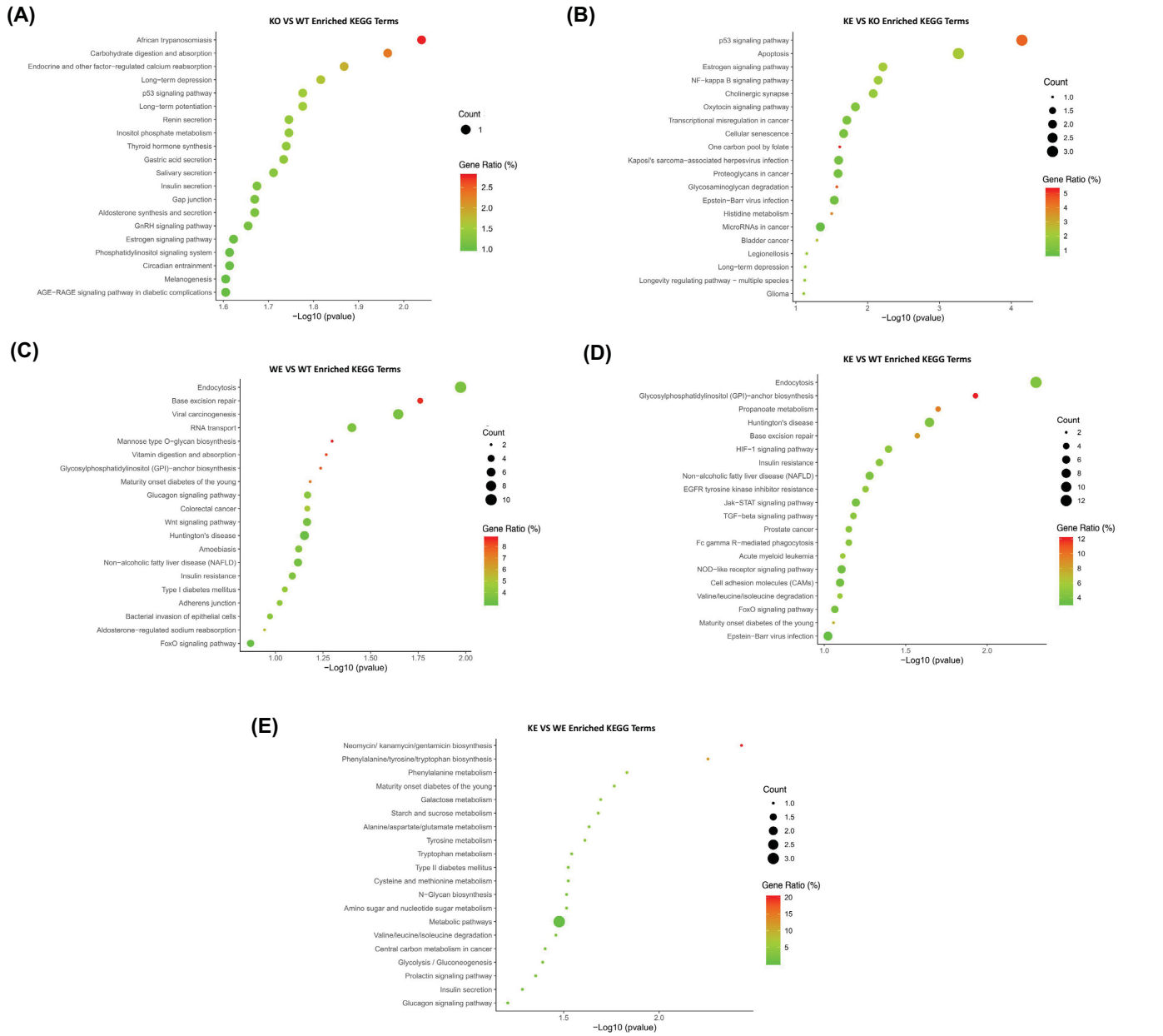

Figure 5. Kyoto Encyclopedia of Genes and Genomes (KEGG) pathways analysis of DEGs

(**A**) KO versus WT, (**B**) KE versus KO, (**C**) WE versus WT, (**D**) KE versus WT, and (**E**) KE versus WE. Dot plots of pathway enrichment analysis were constructed by -log10 (*P* value) and the top 20 KEGG terms. The dot size represents the number of genes enriched in specific KEGG terms, and the dot color represents the gene ratio [i.e. Count (the number of genes enriched) / PopHit (the number of genes annotated)] in specific KEGG terms.

Mtnr1b), identified DEGs (Eps8l1, Plcb2, Chek1, Cdkn1a, Itpr2, Mdm4, Pidd1, Hspa1b), the first-order neighbors of Eps8l1 (Cask, Sos1, Abi1) and Plcb2 (Gna11). As shown in Figure 6F, Asmt may be participated in the molecular mechanism of depression-like behaviors and swimming effects through Bdnf, then Asmt knockout can lead to abnormal expression of Ep8l1 via Sos1. Probably, Asmt knockout play an important role through Mtnr1b/Gna11/Plcb2/Bdnf on depression-like behaviors. Although other identified DEGs from microarray data were not successfully verified by PCR, they may be associated with the pathogenesis of depression and regulation of exercise according to this network.

Bioscience Reports (2022) **42** BSR20220800
https://doi.org/10.1042/BSR20220800

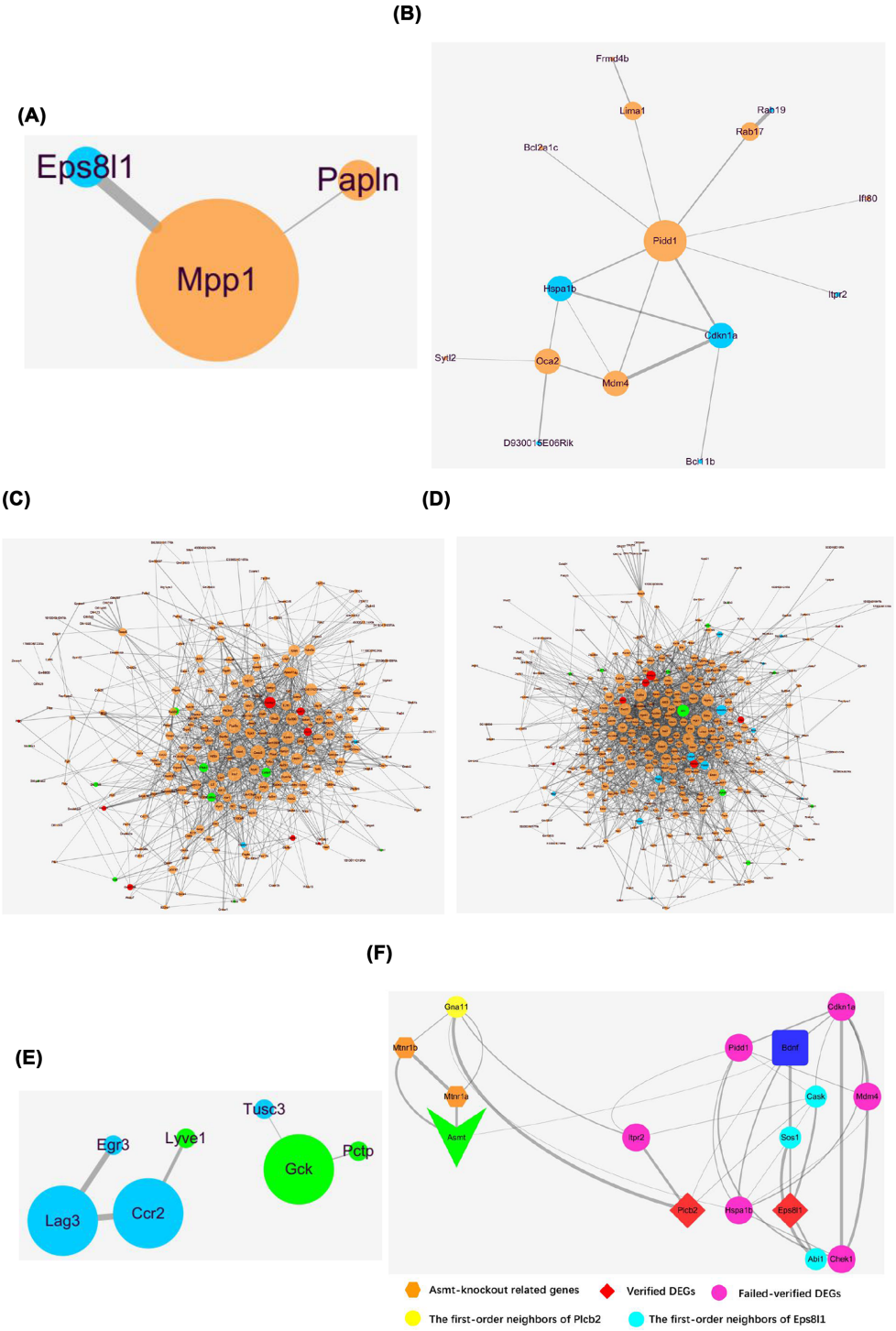

Figure 6. The PPI networks of DEGs

(**A**) KO versus WT, (**B**) KE versus KO, (**C**) WE versus WT, (**D**) KE versus WT, and (**E**) KE versus WE. The PPI networks were constructed by the proteins represented by nodes and interactions represented by the edges between nodes. The nodes size represents the value of degree, and the edge thickness represents the intensity of interactions. Separately, orange and blue nodes represent up-regulated and down-regulated genes, with red and green nodes representing the top 10 up-regulated and down-regulated genes. (**F**) The PPI network was constructed by Asmt, MT receptors (Mtnr1a and Mtnr1b), Bdnf, verified DEGs (Eps8l1 and Plcb2), failed-verified DEGs (Chek1, Cdkn1a, Itpr2, Mdm4, Pidd1, Hspa1b), the first-order neighbors of Eps8l1 (Cask, Sos1, Abi1) and Plcb2 (Gna11). The color and shape of nodes represents different kinds of proteins, and the edge thickness represents the intensity of interactions.

Discussion

To our knowledge, this is the first study to report the animal model of depression induced by Asmt knockout. Of course, it needs further study to confirm the model validity. Initially, we aimed to build Asmt knockout mice to explore the role of MT in depression. However, we ignored the congenital deficiency of Asmt in C57BL/6J mice during gene targeting, thus constructing a mouse strain that seemed to make little sense. Then we thought this question deeply from a different perspective, mouse strain and genotype cannot be ignored when treated with antidepressant therapy [29–31]. Even if C57BL/6J mice were born with melatonin deficiency, genetic deletion of MT1 melatonin receptor caused depressive and anxiety-like behaviors in male and female C57BL/6 mice [32]. In fact, the comparison of different strains of animals showed that the behaviors of C57BL/6J mice in FST, TST, and OFT were similar to other strains [33].

Asmt is the key rate-limiting enzyme of MT [5]. MT has positive effects on depression by regulating neurogenesis [34], neuroplasticity [35], and neurotransmitters [36]. More importantly, MT can improve depression accompanied with anxiety and sleep disorder through oxidative stress and immune response [37]. Therefore, we suppose that Asmt knockout-induced depression-like behaviors may be associated with MT expression. However, Asmt knockout did not significantly affect melatonin levels in our study. Consistently, C57BL/6J mouse strain, which was often used to construct animal models of depression, are inborn with lower Asmt activity in the previous studies. Interestingly, we found that the KE animals show better improvement than WE animals in the behavioral studies, including reduced immobility time in FST ($P<0.01$, Figure 1B) and increased struggling time in FST ($P<0.01$, Figure 1C). It is suggested that male mice with Asmt knockout have an easier time reaping the benefits of exercise than wild-type. The possible explanation for this is that Asmt knockout strengthens neurobehavioral response to exercise due to a significant KO $\times$ swim interaction on the MT level. Furthermore, this may be related to a day-night difference in the response of MT level to swimming [38]. As the substrate of MT formation catalyzed by Asmt, 5-HT is a critical factor linking dysregulation of circadian system and mood [39]. Aerobic exercise has been found to enhance activities of brain serotonergic projections [40]. In the current study, we also found that swimming exercise increased serum 5-HT (i.e. serotonin) level.

To dissect the molecular and genetic basis underlying the association among depression-like behaviors, Asmt knockout and swimming exercise, we have used transcriptome microarray technology. 10 DEGs were identified in mice following Asmt knockout compared with WT group, and 29 DEGs were identified in mice after swimming exercise compared to KO group. Nine DEGs were selected to validate the microarray results, whereas only Eps8l1 and Plcb2 were verified by qRT-PCR. Eps8 has three gene analogs, Eps8l1, Eps8l2, and Eps8l3 [41,42]. Our results showed that Eps8l1 mRNA level in KO group was significantly down-regulated compared to WT group. Similarly, the down-regulation of Eps8 was accompanied by negative effects on cell proliferation, differentiation, and survival [43]. On the contrary, Eps8 has been reported to be up-regulated in most cancer patients, including pituitary gland cancer, breast cancer, ovarian cancer, and so on [44]. Cancer patients have been reported a higher risk of depression [45]. The inconsistency may be due to expression trend in depression and cancer subjects, and also due to expression differences of Eps8 and three analogs. It has been reported that Eps8l1 and Eps8l2, but not Eps8l3, restore receptor tyrosine kinase-dependent actin remodeling and link growth factor stimulation to actin organization [42]. The regulatory effects of Eps8l1 on actin dynamics suggested that it may be connected with exercise intervention for diseases. Consistently, Eps8l1 was one of up-regulated genes after swimming exercise in microarray results. Furthermore, GO terms analysis showed that Eps8l1 was involved in Rac guanyl-nucleotide exchange factor activity, which has been found to regulate glucose metabolism in brain and then relate to brain diseases [46].

Besides, Eps8l1 is crucial for the Eps8-Abi1-Sos1 complex that required for Rac activation leading to actin cytoskeletal remodeling [46]. Sos1 is a guanine nucleotide exchange factor, and Abi1 acts as a scaffold between Eps8 and Sos1 assemble [47]. Cask, another first-order neighbor of Eps8l1, belongs to the membrane-associated guanylate kinase (MAGUK) family, and improve neurodevelopmental disorders by regulating synaptic plasticity [48,49]. These findings suggested that Eps8l1 may be concerned with brain diseases and exercise effects. According to the PPI network (Figure 6F), the effects of Asmt knockout and swimming exercise may be connected with Bdnf, resulting in down-regulation of Eps8l1 via Sos1. Bdnf is important in improving depression-like behaviors by stabilizing hippocampal synaptic plasticity, thus it is the most sensitive neurotrophic factor in antidepressant effects of exercise [50]. Overall, Eps8l1 may take part in molecular mechanism of depression pathology and exercise effects via regulating synaptic plasticity and actin structures.

Plcb2 has been found to mainly distribute in oligodendrocytes and modulate the transmission of neuroendocrine signals [51]. Plcb2 binding to Gna11 is responsible for the regulation of phospholipase C (PLC) in diverse systems [52]. PLC is the key enzyme of phosphatidylinositol signaling pathway, which is closely related to neuron activity

Bioscience Reports (2022) **42** BSR20220800
https://doi.org/10.1042/BSR20220800

and exercise effect. It has been reported that PLC signal disorder is involved in neuropsychiatric diseases including depression, bipolar disorder, schizophrenia, Huntington's disease, and Alzheimer's disease [51]. Six subtypes of PLC have been identified in mammals, namely PLC β, PLC γ, PLC δ, PLC ε, PLC ζ and PLC η. Among them, PLC β is encoded by the Plcb gene, including Plcb1, Plcb2, Plcb3, and Plcb4. Plcb1-related signal pathway related to depression [53], and chronic treatment with quetiapine changed Plcb1 mRNA level from microarray analysis [54]. Our results of enrichment analysis suggested that Plcb2 may be also one of depression-related target molecules like Plcb1. GO terms enriched by Plcb2 mainly included sensory perception of bitter taste, cytoplasm, PLC activity, etc. KEGG terms enriched by Plcb2 included LTD, estrogen signaling pathways, circadian entrainment, melanogenesis, carbohydrate digestion and absorption, and AGE-RAGE signaling pathway in diabetic complications. Our results showed that Plcb2 mRNA level was reduced following Asmt knockout in mice. Consistent with the PPI network (Figure 6F), Asmt knockout may play an important role through Mtnr1b/Gna11/Plcb2/Bdnf in depression. Taken together, Plcb2 may be a representative molecular marker of depression through the effects on circadian rhythm and metabolism, which are crucial for depression [55] and exercise [56].

It is worth noting that MT levels in Asmt KO mice decreased compared with WT mice, but there was no significant difference. If the MT levels were not altered in Asmt KO mice, Eps8l1 and Plcb2 might ameliorate depressive symptoms in a more direct way. After Asmt was knocked out, the mRNA expression levels of Eps8l1 and Plcb2 decreased (Figures 2A,B and 3A,B). Then Eps8l1 can down-regulate Bdnf via Sos1, and Plcb2 can down-regulate Bdnf directly (Figure 6F). This reasonable conjecture is supported by evidence from the previous study. It is reported that Eps8 regulates axonal filopodia in hippocampal neurons in response to Bdnf, this is a process with crucial impacts on neuronal development and synapse formation [57]. The results indicated that 5-HT affected Bdnf secretion from NG2 cells via the PLC signaling pathway [58]. And the cortical oligodendrocytes regulated the release of Bdnf through the PLC pathway [59]. In other words, Eps8l1 and Plcb2 may regulate synaptic plasticity by affecting the expression level of Bdnf to participate in the molecular mechanisms of depression.

In addition, our microarray data show that the RIKEN cDNA 8430408G22 gene, RIKEN cDNA D930015E06 gene, and RIKEN cDNA 1700001P01 gene down-regulated significantly in the antidepressant effects of exercise (Supplementary Table S4). Long non-coding RNA (LncRNA) is defined as a non-coding RNA molecule with a length of more than 200 nucleotides and was initially described by Okazaki et al in a large-scale sequencing study of a full-length mouse cDNA library in 2002. Recently, the roles of lncRNA in the pathogenesis of depression have been shown to regulate synaptic plasticity, Bdnf expression, inflammation and so on [60]. LncRNA networks are differentially modified during endurance exercise in mice with depression-like behaviors [61]. Further, it was confirmed that Baduanjin can effectively ameliorate the symptoms of depression in patients with depression by regulating the dysregulated expression of lncRNA, mRNA, and circRNA [62]. So far, the researchers have raised some predictions of lncRNA function, and their signal pathway and related regulatory networks still need to be further explored in the experiments.

KEGG analysis also revealed that p53 signaling pathway, LTD, and estrogen signaling pathway were enriched significantly following Asmt knockout and swimming exercise. p53 signaling pathway is extremely essential for oxidative stress imposed by exercise [63] and brain development [64,65]. p53 dysfunction was involved in depression and medicating apoptosis [66]. Recently, p53 loss has been found to drive neuron reprogramming in cancer [67]. Consistently, Eps8l1 is also a key molecule in cancer research. These results suggest that there may be a comorbidity between cancer and depression induced by Asmt knockout. LTD pathway is also a kind of synapse plasticity form depending on the change of postsynaptic Ca^{2+} [68]. The increased LTD has been reported to be reversed by antidepressants in rat hippocampal CA1 region [69]. The synaptic plasticity of cortical striatum was involved in learning and exercise control [70]. Additionally, estrogen signaling pathway related to postpartum depression [71]. Women are 2.5 times more likely to suffer from major depressive disorder (MDD) than men, which may due to the reduced estrogen level [72]. Depression is a kind of abnormal disease of brain energy metabolism, the estradiol combining with estrogen receptors can modulate emotion and energy homeostasis through c-fos neural activity in amygdala and hypothalamus [73]. Further study is needed to explore the roles of p53 signaling pathway, LTD and estrogen signaling pathway in Asmt-related depression and exercise effects.

Finally, we identified two hub genes as candidate therapeutic target genes, Mpp1 and Pidd1, which play important roles in PPI networks. Following Asmt knockout in mice, Mpp1 is the core gene in the PPI network. Mpp1 has been reported to regulate neutrophil polarization by AKT1 phosphorylation [74]. Depression can be regarded as an inflammatory disorder, whose pathophysiological mechanism is associated with AKT activity [75]. Mpp1, a skeleton protein in the erythrocyte membrane, belongs to the MAGUK family [76]. Based on the above statements, Mpp1 may be an important target molecule related to depression and exercise effects. After swimming exercise in KO mice, Pidd1 is the core gene in the PPI network. It is reported that Pidd1 may be participated in depression pathogenesis

via Bdnf in the downstream [77]. KEGG terms enriched by Pidd1 included negative regulation of p53 signaling pathway, apoptosis, NF-kappaB signaling pathway, etc. The previous study has found that Pidd1 connected p53/TP53 to apoptosis as a component of DNA damage/stress response pathway [78]. Pidd1 is also important in the activation of NF-kappaB [79]. It has been proposed that the antagonistic relationship between p53 and NF-kappaB may explain the conversion between mania and depression state in bipolar disorders patients [80]. Moreover, exercise effects have been widely studied in regulating NF-kappaB and improving depression.

Asmt knockout induced depression-like behaviors, which were ameliorated by swimming exercise. Our results predicted some meaningful target genes as the biomarkers of depression-like behaviors and swimming exercise. Of these, Eps8l1 and Plcb2 were the first time to be proposed as the target genes in depression. Moreover, they may also be regulated by exercise. In addition, our bioinformatic results showed that p53 signaling pathway, long-term depression and estrogen signaling pathway were enriched significantly. As the hub genes in the PPI networks, the expression of Mpp1 and Pidd1 may provide diagnostic and therapeutic value for depression. Deficiently, the small sample size and differences of RNA extraction methods in different laboratories may affect the results in the present study. In addition, circadian rhythm were not recorded in mice. Consequently, further study is needed to understand the underlying mechanism of these DEGs (including Eps8l1, Plcb2, Mpp1, Pidd1) in Asmt-related depression and exercise effects, thus provide new targets for the treatment of exercise for depression.

In summary, many laboratory mice, including C57BL/6J, are born with lower Asmt activity and MT deficiency due to the mutations at the Asmt. Thus, the idea that MT deficiency causes depression may be not reasonable in C57BL/6J mice. But it may affect the body's response to exercise, which can play an important role in depression treatment. Our results suggest that Asmt and exercise may affect the depression neurobehavior responsiveness in male C57BL/6J mice. Also, the present study concludes that Asmt knockout increase neurobehavioral response to exercise, probably due to changed related gene expression levels. These findings may provide new targets for the treatment of exercise for depression.

Data Availability

The microarray dataset is available at the National Center for Biotechnology Information's Gene Expression Omnibus database (GEO accession: GSE197888).

Competing Interests

The authors declare that there are no competing interests associated with the manuscript.

Funding

This work was supported by the National Natural Science Foundation of China [grant number 31871208]; the Natural Science Foundation of Shanghai [grant number 18ZR1412000]; the Fundamental Research Funds for the Central Universities [grant number 40500-21203-542500/006/004]; and 2021 Excellent Doctoral Student Academic Innovation Ability Enhancement Program of East China Normal University [grant number YBNLTS2021-022].

CRediT Author Contribution

Wenbin Liu: Data curation, Software, Formal analysis, Funding acquisition, Writing—original draft, Project administration, Writing—review & editing. **Zhuochun Huang:** Validation, Investigation. **Jie Xia:** Resources, Supervision. **Zhiming Cui:** Software, Validation. **Lingxia Li:** Investigation. **Zhengtang Qi:** Resources, Supervision, Methodology, Project administration. **Weina Liu:** Conceptualization, Resources, Data curation, Supervision, Funding acquisition, Writing—original draft, Writing—review & editing.

Ethics Approval

All animal experiments were conducted in the Experimental Animal Centre at East China Normal University, Shanghai, China. The details of anaesthetics used and how the animals were sacrificed were showed in the materials and method section of the present article. All procedures were in accordance with the guidelines for the use of laboratory animals published by the People's Republic of China Ministry of Health (No. 55 order, January 25, 1998) and were approved by the Experimental Animal Care and Use Committee at East China Normal University (m20190324), the committee is working as ethics committee to provide approval to the animal studies.

Acknowledgements

We thank all the members for their generous participation.

Abbreviations

5-HT, 5-hydroxytryptamine; Asmt, N-acetyl serotonin methyltransferase; Bdnf, brain-derived neurotrophic factor; BP, biological process; CC, cellular component; Cdkn1a, cyclin-dependent kinase inhibitor 1A; Chek1, checkpoint kinase 1; DEGs, differentially expressed genes; ELISA, enzyme-linked immunosorbent assay; Eps8l1, epidermal growth factor receptor pathway substrate 8-like 1; FST, forced swim test; GO, Gene Ontology; Hspa1b, heat shock protein family A member1B; Itpr2, inositol 1,4,5-triphosphate receptor 2; KEGG, Kyoto Encyclopedia of Genes and Genomes; LTD, long-term depression; Mdm4, transformed mouse 3T3 cell double minute 4; MF, molecular function; Mpp1, membrane palmitoylated protein 1; MT, melatonin; OFT, open field test; Pidd1, p53-induced death domain protein 1; PLC, phospholipase C; Plcb2, phospholipase C-β 2; PPI, protein–protein interaction; qRT-PCR, quantitative real-time polymerase chain reaction; SPT, sucrose preference test; Sytl2, synaptotagmin-like 2.

References

1 Patke, A., Murphy, P.J., Onat, O.E., Krieger, A.C., Ozcelik, T., Campbell, S.S. et al. (2017) Mutation of the human circadian clock gene CRY1 in familial delayed sleep phase disorder. *Cell* **169**, 203–215, https://doi.org/10.1016/j.cell.2017.03.027
2 Burcusa, S.L. and Iacono, W.G. (2007) Risk for recurrence in depression. *Clin. Psychol. Rev.* **27**, 959–985, https://doi.org/10.1016/j.cpr.2007.02.005
3 Marin, H. and Menza, M.A. (2004) Specific treatment of residual fatigue in depressed patients. *Psychiatry (Edgmont)* **1**, 12–18
4 Dale, E., Bang-Andersen, B. and Sanchez, C. (2015) Emerging mechanisms and treatments for depression beyond SSRIs and SNRIs. *Biochem. Pharmacol.* **95**, 81–97, https://doi.org/10.1016/j.bcp.2015.03.011
5 Botros, H.G., Legrand, P., Pagan, C., Bondet, V., Weber, P., Ben-Abdallah, M. et al. (2013) Crystal structure and functional mapping of human ASMT, the last enzyme of the melatonin synthesis pathway. *J. Pineal Res.* **54**, 46–57, https://doi.org/10.1111/j.1600-079X.2012.01020.x
6 Carvalho, L.A., Gorenstein, C., Moreno, R.A. and Markus, R.P. (2006) Melatonin levels in drug-free patients with major depression from the southern hemisphere. *Psychoneuroendocrino* **31**, 761–768, https://doi.org/10.1016/j.psyneuen.2006.02.010
7 Sun, X., Wang, M., Wang, Y., Lian, B., Sun, H., Wang, G. et al. (2017) Melatonin produces a rapid onset and prolonged efficacy in reducing depression-like behaviors in adult rats exposed to chronic unpredictable mild stress. *Neurosci. Lett.* **642**, 129–135, https://doi.org/10.1016/j.neulet.2017.01.015
8 Kripke, D.F., Nievergelt, C.M., Tranah, G.J., Murray, S.S., Mccarthy, M.J., Rex, K.M. et al. (2011) Polymorphisms in melatonin synthesis pathways: possible influences on depression. *J. Circadian Rhythms* **9**, 8, https://doi.org/10.1186/1740-3391-9-8
9 Talarowska, M., Szemraj, J., Zajaczkowska, M. and Galecki, P. (2014) ASMT gene expression correlates with cognitive impairment in patients with recurrent depressive disorder. *Med. Sci. Monit.* **20**, 905–912, https://doi.org/10.12659/MSM.890160
10 Melke, J., Goubran, B.H., Chaste, P., Betancur, C., Nygren, G., Anckarsater, H. et al. (2008) Abnormal melatonin synthesis in autism spectrum disorders. *Mol. Psychiatry* **13**, 90–98, https://doi.org/10.1038/sj.mp.4002016
11 Etain, B., Dumaine, A., Bellivier, F., Pagan, C., Francelle, L., Goubran-Botros, H. et al. (2012) Genetic and functional abnormalities of the melatonin biosynthesis pathway in patients with bipolar disorder. *Hum. Mol. Genet.* **21**, 4030–4037, https://doi.org/10.1093/hmg/dds227
12 Atkinson, G., Edwards, B., Reilly, T. and Waterhouse, J. (2007) Exercise as a synchroniser of human circadian rhythms: an update and discussion of the methodological problems. *Eur. J. Appl. Physiol.* **99**, 331–341, https://doi.org/10.1007/s00421-006-0361-z
13 Yamanaka, Y., Hashimoto, S., Masubuchi, S., Natsubori, A., Nishide, S.Y., Honma, S. et al. (2014) Differential regulation of circadian melatonin rhythm and sleep-wake cycle by bright lights and nonphotic time cues in humans. *Am. J. Physiol. Regul. Integr. Comp. Physiol.* **307**, R546–R557, https://doi.org/10.1152/ajpregu.00087.2014
14 Escames, G., Ozturk, G., Bano-Otalora, B., Pozo, M.J., Madrid, J.A., Reiter, R.J. et al. (2012) Exercise and melatonin in humans: reciprocal benefits. *J. Pineal Res.* **52**, 1–11, https://doi.org/10.1111/j.1600-079X.2011.00924.x
15 Toups, M., Carmody, T., Greer, T., Rethorst, C., Grannemann, B. and Trivedi, M.H. (2017) Exercise is an effective treatment for positive valence symptoms in major depression. *J. Affect. Disord.* **209**, 188–194, https://doi.org/10.1016/j.jad.2016.08.058
16 Michiels, S., Koscielny, S. and Hill, C. (2005) Prediction of cancer outcome with microarrays: a multiple random validation strategy. *Lancet* **365**, 488–492, https://doi.org/10.1016/S0140-6736(05)17866-0
17 Uriguen, L., Arteta, D., Diez-Alarcia, R., Ferrer-Alcon, M., Diaz, A., Pazos, A. et al. (2008) Gene expression patterns in brain cortex of three different animal models of depression. *Genes Brain Behav.* **7**, 649–658, https://doi.org/10.1111/j.1601-183X.2008.00402.x
18 Ronn, T., Volkov, P., Tornberg, A., Elgzyri, T., Hansson, O., Eriksson, K.F. et al. (2014) Extensive changes in the transcriptional profile of human adipose tissue including genes involved in oxidative phosphorylation after a 6-month exercise intervention. *Acta. Physiol. (Oxf.)* **211**, 188–200, https://doi.org/10.1111/apha.12247
19 Muzio, L., Brambilla, V., Calcaterra, L., D'Adamo, P., Martino, G. and Benedetti, F. (2016) Increased neuroplasticity and hippocampal microglia activation in a mice model of rapid antidepressant treatment. *Behav. Brain Res.* **311**, 392–402, https://doi.org/10.1016/j.bbr.2016.05.063
20 Redman, M., King, A., Watson, C. and King, D. (2016) What is CRISPR/Cas9? *Arch. Dis. Child Educ. Pract. Ed.* **101**, 213–215, https://doi.org/10.1136/archdischild-2016-310459
21 Slomka, M., Sobalska-Kwapis, M., Wachulec, M., Bartosz, G. and Strapagiel, D. (2017) High resolution melting (HRM) for high-throughput genotyping-limitations and caveats in practical case studies. *Int. J. Mol. Sci.* **18**, 2316–2334, https://doi.org/10.3390/ijms18112316
22 Liu, W., Xue, X., Xia, J., Liu, J. and Qi, Z. (2018) Swimming exercise reverses CUMS-induced changes in depression-like behaviors and hippocampal plasticity-related proteins. *J. Affect. Disord.* **227**, 126–135, https://doi.org/10.1016/j.jad.2017.10.019

23 Jiang, P., Dang, R.L., Li, H.D., Zhang, L.H., Zhu, W.Y., Xue, Y. et al. (2014) The impacts of swimming exercise on hippocampal expression of neurotrophic factors in rats exposed to chronic unpredictable mild stress. *Evid. Based Complement. Alternat. Med.* **2014**, 729827, https://doi.org/10.1155/2014/729827
24 Liu, W., Liu, J., Huang, Z., Cui, Z., Li, L., Liu, W. et al. (2019) Possible role of GLP-1 in antidepressant effects of metformin and exercise in CUMS mice. *J. Affect. Disord.* **246**, 486–497, https://doi.org/10.1016/j.jad.2018.12.112
25 Sedaghat, K., Yousefian, Z., Vafaei, A.A., Rashidy-Pour, A., Parsaei, H., Khaleghian, A. et al. (2019) Mesolimbic dopamine system and its modulation by vitamin D in a chronic mild stress model of depression in the rat. *Behav. Brain Res.* **356**, 156–169, https://doi.org/10.1016/j.bbr.2018.08.020
26 Petit-Demouliere, B., Chenu, F. and Bourin, M. (2005) Forced swimming test in mice: a review of antidepressant activity. *Psychopharmacology (Berl.)* **177**, 245–255, https://doi.org/10.1007/s00213-004-2048-7
27 Shyong, Y.J., Wang, M.H., Kuo, L.W., Su, C.F., Kuo, W.T., Chang, K.C. et al. (2017) Mesoporous hydroxyapatite as a carrier of olanzapine for long-acting antidepression treatment in rats with induced depression. *J. Control. Release* **255**, 62–72, https://doi.org/10.1016/j.jconrel.2017.03.399
28 Sudheimer, K., Keller, J., Gomez, R., Tennakoon, L., Reiss, A., Garrett, A. et al. (2015) Decreased hypothalamic functional connectivity with subgenual cortex in psychotic major depression. *Neuropsychopharmacol* **40**, 849–860, https://doi.org/10.1038/npp.2014.259
29 Can, A., Blackwell, R.A., Piantadosi, S.C., Dao, D.T., O'Donnell, K.C. and Gould, T.D. (2011) Antidepressant-like responses to lithium in genetically diverse mouse strains. *Genes Brain Behav.* **10**, 434–443, https://doi.org/10.1111/j.1601-183X.2011.00682.x
30 Ripoll, N., David, D.J., Dailly, E., Hascoet, M. and Bourin, M. (2003) Antidepressant-like effects in various mice strains in the tail suspension test. *Behav. Brain Res.* **143**, 193–200, https://doi.org/10.1016/S0166-4328(03)00034-2
31 Tang, M., He, T., Meng, Q.Y., Broussard, J.I., Yao, L., Diao, Y. et al. (2014) Immobility responses between mouse strains correlate with distinct hippocampal serotonin transporter protein expression and function. *Int. J. Neuropsychopharmacol.* **17**, 1737–1750, https://doi.org/10.1017/S146114571400073X
32 Adamah-Biassi, E.B., Hudson, R.L. and Dubocovich, M.L. (2014) Genetic deletion of MT1 melatonin receptors alters spontaneous behavioral rhythms in male and female C57BL/6 mice. *Horm. Behav.* **66**, 619–627, https://doi.org/10.1016/j.yhbeh.2014.08.012
33 Lockridge, A., Newland, B., Printen, S., Romero, G.E. and Yuan, L.L. (2013) Head movement: a novel serotonin-sensitive behavioral endpoint for tail suspension test analysis. *Behav. Brain Res.* **246**, 168–178, https://doi.org/10.1016/j.bbr.2013.02.032
34 Crupi, R., Mazzon, E., Marino, A., La Spada, G., Bramanti, P., Cuzzocrea, S. et al. (2010) Melatonin treatment mimics the antidepressant action in chronic corticosterone-treated mice. *J. Pineal Res.* **49**, 123–129, https://doi.org/10.1111/j.1600-079X.2010.00775.x
35 Valdes-Tovar, M., Estrada-Reyes, R., Solis-Chagoyan, H., Argueta, J., Dorantes-Barron, A.M., Quero-Chavez, D. et al. (2018) Circadian modulation of neuroplasticity by melatonin: a target in the treatment of depression. *Br. J. Pharmacol.* **175**, 3200–3208, https://doi.org/10.1111/bph.14197
36 Weil, Z.M., Hotchkiss, A.K., Gatien, M.L., Pieke-Dahl, S. and Nelson, R.J. (2006) Melatonin receptor (MT1) knockout mice display depression-like behaviors and deficits in sensorimotor gating. *Brain Res. Bull.* **68**, 425–429, https://doi.org/10.1016/j.brainresbull.2005.09.016
37 Zhang, R., Wang, X., Ni, L., Di, X., Ma, B., Niu, S. et al. (2020) COVID-19: Melatonin as a potential adjuvant treatment. *Life Sci.* **250**, 117583, https://doi.org/10.1016/j.lfs.2020.117583
38 Wu, W.T., Chen, Y.C. and Reiter, R.J. (1988) Day-night differences in the response of the pineal gland to swimming stress. *Proc. Soc. Exp. Biol. Med.* **187**, 315–319, https://doi.org/10.3181/00379727-187-42670
39 Daut, R.A. and Fonken, L.K. (2019) Circadian regulation of depression: a role for serotonin. *Front. Neuroendocrinol.* **54**, 100746, https://doi.org/10.1016/j.yfrne.2019.04.003
40 Melancon, M.O., Lorrain, D. and Dionne, I.J. (2014) Exercise and sleep in aging: emphasis on serotonin. *Pathol. Biol. (Paris)* **62**, 276–283, https://doi.org/10.1016/j.patbio.2014.07.004
41 Ion, A., Crosby, A.H., Kremer, H., Kenmochi, N., Van Reen, M., Fenske, C. et al. (2000) Detailed mapping, mutation analysis, and intragenic polymorphism identification in candidate Noonan syndrome genes MYL2, DCN, EPS8, and RPL6. *J. Med. Genet.* **37**, 884–886, https://doi.org/10.1136/jmg.37.11.884
42 Offenhauser, N., Borgonovo, A., Disanza, A., Romano, P., Ponzanelli, I., Iannolo, G. et al. (2004) The eps8 family of proteins links growth factor stimulation to actin reorganization generating functional redundancy in the Ras/Rac pathway. *Mol. Biol. Cell* **15**, 91–98, https://doi.org/10.1091/mbc.e03-06-0427
43 Satoh, J., Kuroda, Y. and Katamine, S. (2000) Gene expression profile in prion protein-deficient fibroblasts in culture. *Am. J. Pathol.* **157**, 59–68, https://doi.org/10.1016/S0002-9440(10)64517-8
44 Welsch, T., Younsi, A., Disanza, A., Rodriguez, J.A., Cuervo, A.M., Scita, G. et al. (2010) Eps8 is recruited to lysosomes and subjected to chaperone-mediated autophagy in cancer cells. *Exp. Cell. Res.* **316**, 1914–1924, https://doi.org/10.1016/j.yexcr.2010.02.020
45 Sotelo, J.L., Musselman, D. and Nemeroff, C. (2014) The biology of depression in cancer and the relationship between depression and cancer progression. *Int. Rev. Psychiatry* **26**, 16–30, https://doi.org/10.3109/09540261.2013.875891
46 Hong, J., Kim, Y., Yanpallewar, S. and Lin, P.C. (2020) The Rho/Rac guanine nucleotide exchange factor Vav1 regulates Hif-1alpha and Glut-1 expression and glucose uptake in the brain. *Int. J. Mol. Sci.* **21**, 1341–1350, https://doi.org/10.3390/ijms21041341
47 Scita, G., Nordstrom, J., Carbone, R., Tenca, P., Giardina, G., Gutkind, S. et al. (1999) EPS8 and E3B1 transduce signals from Ras to Rac. *Nature* **401**, 290–293, https://doi.org/10.1038/45822
48 Hsueh, Y.P. (2006) The role of the MAGUK protein CASK in neural development and synaptic function. *Curr. Med. Chem.* **13**, 1915–1927, https://doi.org/10.2174/092986706777585040
49 Zheng, C.Y., Seabold, G.K., Horak, M. and Petralia, R.S. (2011) MAGUKs, synaptic development, and synaptic plasticity. *Neuroscientist* **17**, 493–512, https://doi.org/10.1177/1073858410386384
50 Qiao, H., An, S.C., Xu, C. and Ma, X.M. (2017) Role of proBDNF and BDNF in dendritic spine plasticity and depressive-like behaviors induced by an animal model of depression. *Brain Res.* **1663**, 29–37, https://doi.org/10.1016/j.brainres.2017.02.020

51 Yang, Y.R., Kang, D.S., Lee, C., Seok, H., Follo, M.Y., Cocco, L. et al. (2016) Primary phospholipase C and brain disorders. *Adv. Biol. Regul.* **61**, 80–85, https://doi.org/10.1016/j.jbior.2015.11.003
52 Gutowski, S., Smrcka, A., Nowak, L., Wu, D.G., Simon, M. and Sternweis, P.C. (1991) Antibodies to the alpha q subfamily of guanine nucleotide-binding regulatory protein alpha subunits attenuate activation of phosphatidylinositol 4,5-bisphosphate hydrolysis by hormones. *J. Biol. Chem.* **266**, 20519–20524, https://doi.org/10.1016/S0021-9258(18)54955-3
53 Kao, C.F., Jia, P., Zhao, Z. and Kuo, P.H. (2012) Enriched pathways for major depressive disorder identified from a genome-wide association study. *Int. J. Neuropsychopharmacol.* **15**, 1401–1411, https://doi.org/10.1017/S1461145711001891
54 Orsetti, M., Di Brisco, F., Rinaldi, M., Dallorto, D. and Ghi, P. (2009) Some molecular effectors of antidepressant action of quetiapine revealed by DNA microarray in the frontal cortex of anhedonic rats. *Pharmacogenet. Genomics* **19**, 600–612, https://doi.org/10.1097/FPC.0b013e32832ee573
55 Liu, W., Wang, Y., Li, H. and Ji, L. (2016) The role of nitric oxide in the antidepressant actions of 5-aminoimidazole-4-carboxamide-1-beta-D-ribofuranoside in insulin-resistant mice. *Psychosom. Med.* **78**, 102–112, https://doi.org/10.1097/PSY.0000000000000268
56 Tahara, Y., Aoyama, S. and Shibata, S. (2017) The mammalian circadian clock and its entrainment by stress and exercise. *J. Physiol. Sci.* **67**, 1–10, https://doi.org/10.1007/s12576-016-0450-7
57 Menna, E., Disanza, A., Cagnoli, C., Schenk, U., Gelsomino, G., Frittoli, E. et al. (2009) Eps8 regulates axonal filopodia in hippocampal neurons in response to brain-derived neurotrophic factor (BDNF). *PLoS Biol.* **7**, e1000138, https://doi.org/10.1371/journal.pbio.1000138
58 Yang, T., Li, Y., Wang, H., Shi, P., Teng, L., Guo, H. et al. (2022) The 5-HT and PLC signaling pathways regulate the secretion of IL-1beta, TNF-alpha and BDNF from NG2 cells. *Evid. Based Complement Alternat. Med.* **2022**, 7425538, https://doi.org/10.1155/2022/7425538
59 Bagayogo, I.P. and Dreyfus, C.F. (2009) Regulated release of BDNF by cortical oligodendrocytes is mediated through metabotropic glutamate receptors and the PLC pathway. *ASN Neuro.* **1**, e00001, https://doi.org/10.1042/AN20090006
60 Liu, N., Wang, Z.Z., Zhao, M., Zhang, Y. and Chen, N.H. (2020) Role of non-coding RNA in the pathogenesis of depression. *Gene* **735**, 144276, https://doi.org/10.1016/j.gene.2019.144276
61 Abedpoor, N., Taghian, F. and Hajibabaie, F. (2022) Cross brain-gut analysis highlighted hub genes and LncRNA networks differentially modified during leucine consumption and endurance exercise in mice with depression-like behaviors. *Mol. Neurobiol.* **59**, 4106–4123, https://doi.org/10.1007/s12035-022-02835-1
62 An, T., He, Z.C., Zhang, X.Q., Li, J., Chen, A.L., Tan, F. et al. (2019) Baduanjin exerts anti-diabetic and anti-depression effects by regulating the expression of mRNA, lncRNA, and circRNA. *Chin Med* **14**, 3, https://doi.org/10.1186/s13020-019-0225-1
63 Beyfuss, K. and Hood, D.A. (2018) A systematic review of p53 regulation of oxidative stress in skeletal muscle. *Redox Rep.* **23**, 100–117, https://doi.org/10.1080/13510002.2017.1416773
64 Holley, A.K. and St, C.D. (2009) Watching the watcher: regulation of p53 by mitochondria. *Fut. Oncol.* **5**, 117–130, https://doi.org/10.2217/14796694.5.1.117
65 Smeenk, L., van Heeringen, S.J., Koeppel, M., van Driel, M.A., Bartels, S.J., Akkers, R.C. et al. (2008) Characterization of genome-wide p53-binding sites upon stress response. *Nucleic Acids Res.* **36**, 3639–3654, https://doi.org/10.1093/nar/gkn232
66 Wang, F., Wang, J., An, J., Yuan, G., Hao, X. and Zhang, Y. (2018) Resveratrol ameliorates depressive disorder through the NETRIN1-mediated extracellular signal-regulated kinase/cAMP signal transduction pathway. *Mol. Med. Rep.* **17**, 4611–4618
67 Amit, M., Takahashi, H., Dragomir, M.P., Lindemann, A., Gleber-Netto, F.O., Pickering, C.R. et al. (2020) Loss of p53 drives neuron reprogramming in head and neck cancer. *Nature* **578**, 449–454, https://doi.org/10.1038/s41586-020-1996-3
68 Zamora, C.C. and De Schutter, E. (2018) Ca(2+) requirements for long-term depression are frequency sensitive in Purkinje cells. *Front. Mol. Neurosci.* **11**, 438, https://doi.org/10.3389/fnmol.2018.00438
69 Collingridge, G.L., Peineau, S., Howland, J.G. and Wang, Y.T. (2010) Long-term depression in the CNS. *Nat. Rev. Neurosci.* **11**, 459–473, https://doi.org/10.1038/nrn2867
70 Ma, J., Chen, H., Liu, X., Zhang, L. and Qiao, D. (2018) Exercise-induced fatigue impairs bidirectional corticostriatal synaptic plasticity. *Front. Cell. Neurosci.* **12**, 14, https://doi.org/10.3389/fncel.2018.00014
71 Zhang, S., Hong, J., Zhang, T., Wu, J. and Chen, L. (2017) Activation of sigma-1 receptor alleviates postpartum estrogen withdrawal-induced "depression" through restoring hippocampal nNOS-NO-CREB activities in mice. *Mol. Neurobiol.* **54**, 3017–3030, https://doi.org/10.1007/s12035-016-9872-8
72 Chhibber, A., Woody, S.K., Karim, R.M., Soares, M.J. and Zhao, L. (2017) Estrogen receptor beta deficiency impairs BDNF-5-HT2A signaling in the hippocampus of female brain: a possible mechanism for menopausal depression. *Psychoneuroendocrino* **82**, 107–116, https://doi.org/10.1016/j.psyneuen.2017.05.016
73 Estrada, C.M., Ghisays, V., Nguyen, E.T., Caldwell, J.L., Streicher, J. and Solomon, M.B. (2018) Estrogen signaling in the medial amygdala decreases emotional stress responses and obesity in ovariectomized rats. *Horm. Behav.* **98**, 33–44, https://doi.org/10.1016/j.yhbeh.2017.12.002
74 Quinn, B.J., Welch, E.J., Kim, A.C., Lokuta, M.A., Huttenlocher, A., Khan, A.A. et al. (2009) Erythrocyte scaffolding protein p55/MPP1 functions as an essential regulator of neutrophil polarity. *Proc. Natl. Acad. Sci. U. S. A.* **106**, 19842–19847, https://doi.org/10.1073/pnas.0906761106
75 Coyle, J.T. and Duman, R.S. (2003) Finding the intracellular signaling pathways affected by mood disorder treatments. *Neuron* **38**, 157–160, https://doi.org/10.1016/S0896-6273(03)00195-8
76 Trybus, M., Niemiec, L., Biernatowska, A., Hryniewicz-Jankowska, A. and Sikorski, A.F. (2019) MPP1-based mechanism of resting state raft organization in the plasma membrane. Is it a general or specialized mechanism in erythroid cells? *Folia. Histochem. Cytobiol.* **57**, 43–55, https://doi.org/10.5603/FHC.a2019.0007
77 Caviedes, A., Lafourcade, C., Soto, C. and Wyneken, U. (2017) BDNF/NF-kappaB signaling in the neurobiology of depression. *Curr. Pharm. Des.* **23**, 3154–3163, https://doi.org/10.2174/1381612823666170111141915

78 Kim, I.R., Murakami, K., Chen, N.J., Saibil, S.D., Matysiak-Zablocki, E., Elford, A.R. et al. (2009) DNA damage- and stress-induced apoptosis occurs independently of PIDD. *Apoptosis* **14**, 1039–1049, https://doi.org/10.1007/s10495-009-0375-1

79 Bock, F.J., Krumschnabel, G., Manzl, C., Peintner, L., Tanzer, M.C., Hermann-Kleiter, N. et al. (2013) Loss of PIDD limits NF-kappaB activation and cytokine production but not cell survival or transformation after DNA damage. *Cell Death Differ.* **20**, 546–557, https://doi.org/10.1038/cdd.2012.152

80 Morris, G., Walder, K., Mcgee, S.L., Dean, O.M., Tye, S.J., Maes, M. et al. (2017) A model of the mitochondrial basis of bipolar disorder. *Neurosci. Biobehav. Rev.* **74**, 1–20, https://doi.org/10.1016/j.neubiorev.2017.01.014

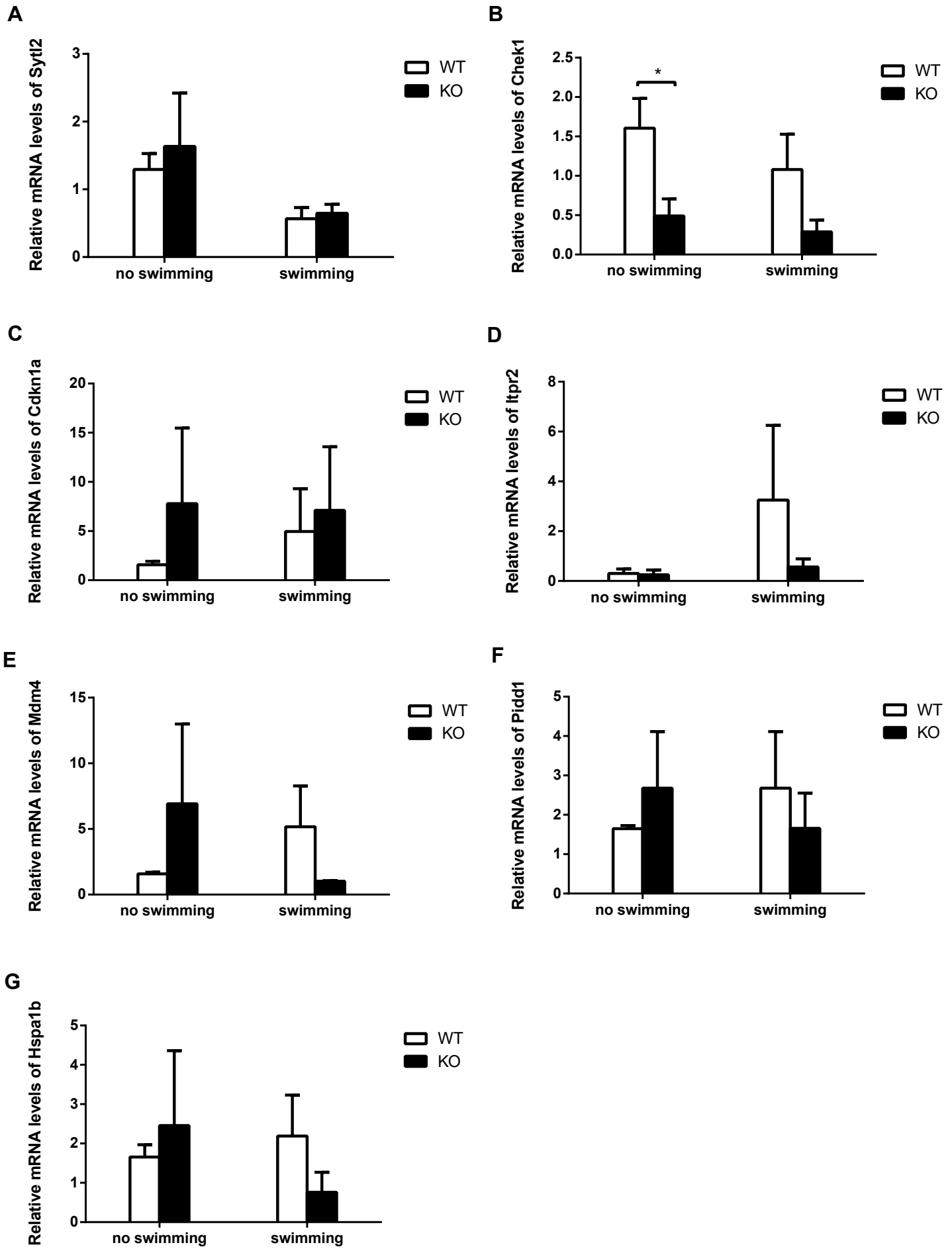
A
Relative mRNA levels of Sytl2
3
2
1
0
WT
KO
no swimming
swimming
B
Relative mRNA levels of Chek1
2.5
2.0
1.5
1.0
0.5
0.0
*
WT
KO
no swimming
swimming
C
Relative mRNA levels of Cdkn1a
20
15
10
5
0
WT
KO
no swimming
swimming
D
Relative mRNA levels of Itpr2
8
6
4
2
0
WT
KO
no swimming
swimming
E
Relative mRNA levels of Mdm4
15
10
5
0
WT
KO
no swimming
swimming
F
Relative mRNA levels of Pidd1
5
4
3
2
1
0
WT
KO
no swimming
swimming
G
Relative mRNA levels of Hspa1b
5
4
3
2
1
0
WT
KO
no swimming
swimming

Figure S1

Figure S1. Validation of DEGs by qRT-PCR. The expression levels of the other seven genes in hypothalamus in response to Asmt knockout and swimming exercise. (A) synaptotagmin-like 2 (Styl2), (B) checkpoint kinase 1 (Chek1), (C) cyclin-dependent kinase inhibitor 1a (Cdkn1a), (D) inositol 1,4,5-triphosphate receptor 2 (Itpr2), (E) transformed mouse 3T3 cell double minute 4 (Mdm4), (F) p53 induced death domain protein 1 (Pidd1), and (G) heat shock protein 1b (Hspa1b). The relative mRNA levels was conducted using qRT-PCR. Data are presented as means ± SEM (n = 3 per group). * $p < 0.05$ versus WT.

Supplementary Table 1. Gene-specific primers for quantitative real-time PCR.

Primer name	Sequence
Eps8l1	F: 5’-TCATTTGATCCCGGCTCGAT-3’
	R: 5’-TCCCTTTCCCCATTCCCATC-3’
Plcb2	F: 5’-CTCTTCTCCTGTCCCCTGG-3’
	R: 5’-TCTGCAAAGCTCCCAAGC-3’
Sytl2	F: 5’-GGCCTAACCATCCACGAGAG-3’
	R: 5’-GAATCGCTTGGGCTTGACAC-3’
Chek1	F: 5’-GAGAAAGGGAATTCTGAGGTG-3’
	R: 5’-TGGTGGGTTTAATGTCCAGC-3’
Cdkn1a	F: 5’-GGTGGGCTTATCTGGGATGG-3’
	R: 5’-AAACAGGGATGTTTGGGGCT-3’
Itpr2	F: 5’-GGAAGAGAGGCCTGTCATGT-3’
	R: 5’-GTGATGCTGCCATTCTCCAG-3’
Mdm4	F: 5’-GATCCTCCTGCCTGGCTTAC-3’
	R: 5’-CACAGACAGTGCATGCAGAC-3’
Pidd1	F: 5’-CTTTGTCCCTCCACGAGTCC-3’
	R: 5’-CCTGAGGAGCAGAGAAGTGC-3’
Hspa1b	F: 5’-CTGCTTGGGCACCGATTACT-3’
	R: 5’-TCCCAGGCTACTGGAACACT-3’
18S	F: 5’-GTAACCCGTTGAACCCCATT-3’
	R: 5’-CCATCCAATCGGTAGTAGCG-3’

Supplementary Table 2. The overall results of DEGs.

Comparison	Up-regulated DEGs	Down-regulated DEGs	Total
KO VS WT	7	3	10
KE VS KO	17	12	29
WE VS WT	359	17	376
KE VS WT	455	29	484
KE VS WE	6	18	24

Supplementary Table 3. The DEGs between the KO and WT groups.

Gene symbol	Gene name	*P* value	Fold change	RefSeq gene name
Up-regulated genes				
Mpp1	membrane palmitoylated protein 1	0.00806796	3.17	AK165261
Tspan1	tetraspanin 1	0.00955007	3.80	NM_133681
Chek1	checkpoint kinase 1	0.01303070	2.13	NM_007691
Tns4	tensin 4	0.01873418	2.06	/
Evx2	even skipped homeotic gene 2 homolog	0.03593857	2.18	NM_007967
Teddm2	transmembrane epididymal family member 2	0.03639276	2.31	NM_178243
Papln	proteoglycan-like sulfated glycoprotein	0.04980407	2.11	NM_001205343
Down-regulated genes				
Eps8l1	EPS8-like 1	0.00422430	-3.77	NM_026146
Plcb2	phospholipase C, beta 2	0.01100710	-8.11	NM_177568
Sytl2	synaptotagmin-like 2	0.03631679	-2.35	NR_110348

Supplementary Table 4. The DEGs between the KE and KO groups.

Gene symbol	Gene name	*P* value	Fold change	RefSeq gene name
Up-regulated genes				
Ift80	intraflagellar transport 80	0.00142910	5.60	NM_026641
Plekho2	pleckstrin homology domain containing, family O member 2	0.00238690	2.15	AK172714
Eps8l1	EPS8-like 1	0.00304345	3.97	NM_026146
Oca2	oculocutaneous albinism II	0.00556511	5.86	NM_021879
Rab17	RAB17, member RAS oncogene family	0.00856209	4.51	NM_008998
Slc16a8	solute carrier family 16 (monocarboxylic acid transporters), member 8	0.01601820	2.01	NM_020516
Lima1	LIM domain and actin binding 1	0.01671470	2.62	AK028311
Tbc1d23	TBC1 domain family, member 23	0.02440666	2.01	AK028852
Tmem192	transmembrane protein 192	0.02603117	2.16	AK090347
Mdm4	transformed mouse 3T3 cell double minute 4	0.02605572	2.18	AK028493
Slfn9	schlafen 9	0.02928562	2.36	NM_172796
Pidd1	p53 induced death domain protein 1	0.03002435	2.04	XM_006536220
Frmd4b	FERM domain containing 4B	0.03248306	2.09	AK051779
Kcnq5	potassium voltage-gated channel, subfamily Q, member 5	0.03835360	2.55	/
Sytl2	synaptotagmin-like 2	0.03854868	2.45	NR_110348
Bcl2a1c	B cell leukemia/lymphoma 2 related protein A1c	0.04754736	2.03	NM_007535
Glra3	glycine receptor, alpha 3 subunit	0.04915356	2.59	AK038618
Down-regulated genes				
8430408G22Rik	RIKEN cDNA 8430408G22 gene	0.00433508	-2.71	NM_145980
Hyal2	hyaluronoglucosaminidase 2	0.00851087	-3.08	AK087358
Gm1070	predicted gene 1070	0.01415500	-2.72	XR_105056
Bcl11b	B cell leukemia/lymphoma 11B	0.01569456	-2.09	XM_006516114
D930015E06Rik	RIKEN cDNA D930015E06 gene	0.02218209	-2.27	NM_172681
Rab19	RAB19, member RAS oncogene family	0.02307621	-2.29	NM_011226
1700001P01Rik	RIKEN cDNA 1700001P01 gene	0.02428712	-2.30	NM_028156
Ftcd	formiminotransferase cyclodeaminase	0.03222452	-2.18	NM_080845
Itpr2	inositol 1,4,5-triphosphate receptor 2	0.03246053	-2.31	/
Cdkn1a	cyclin-dependent kinase inhibitor 1A (P21)	0.03963165	-2.07	NM_007669
Hspa1b	heat shock protein 1B	0.04467700	-2.03	NM_010478
Veph1	ventricular zone expressed PH domain-containing 1	0.04984868	-2.14	NM_145820

Supplementary Table 5. The top 10 DEGs between the WE and WT groups.

Gene symbol	Gene name	*P* value	Fold change	RefSeq gene name
Up-regulated genes				
Gm4788	predicted gene 4788	0.00000243	7.46	NM_001029977
Lrp1b	low density lipoprotein-related protein 1B	0.00000593	6.59	XM_006498459
Ranbp1	RAN binding protein 1	0.00000763	4.28	AK151167
Bex6	brain expressed gene 6	0.00001760	8.10	NM_001033539
Pigb	phosphatidylinositol glycan anchor biosynthesis, class B	0.00001830	2.67	AK161911
Spry4	sprouty homolog 4	0.00002970	8.60	NM_011898
Nudt19	nucleoside diphosphate linked moiety X-type motif 19	0.00003460	2.16	NM_033080
Ttc34	tetratricopeptide repeat domain 34	0.00003540	4.03	XM_006538862
Spint2	hepatocyte growth factor activator inhibitor type 2 (Hai2)	0.00004560	5.34	AF099016
H2-Q1	histocompatibility 2, Q region locus 1	0.00005890	2.96	NM_010390
Down-regulated genes				
Slc17a9	solute carrier family 17, member 9	0.00078700	-2.29	BC019537
Krt6a	keratin 6A	0.00364642	-3.32	NM_008476
St6galnac 2	ST6(alpha-N-acetyl-neuraminyl-2,3-beta-galactosyl-1,3)-N-acetylgalactosaminide alpha-2,6-sialyltransferase 2	0.00383534	-2.04	NM_009180
Slc35b3	solute carrier family 35, member B3	0.00445461	-2.48	AK167051
Plcb2	phospholipase C, beta 2	0.00472553	-10.15	NM_177568
Col6a2	collagen, type VI, alpha 2	0.00527168	-2.98	AK044870
Gls	glutaminase	0.01436419	-2.03	AK046297
Cabp5	calcium binding protein 5	0.01656183	-2.08	NM_013877
Veph1	ventricular zone expressed PH domain-containing 1	0.02253773	-2.37	NM_145820
Lrat	lecithin-retinol acyltransferase (phosphatidylcholine-retinol-O-acyltransferase)	0.03409176	-2.03	NM_023624

Supplementary Table 6. The top 10 DEGs between the KE and WT groups.

Gene symbol	Gene name	*P* value	Fold change	RefSeq gene name
Up-regulated genes				
Slc51b	solute carrier family 51, beta subunit	0.00000138	5.70	NM_178933
Bex6	brain expressed gene 6	0.00000160	8.47	NM_001033539
Gfra4	glial cell line derived neurotrophic factor family receptor alpha 4	0.00000314	2.28	NM_001271002
Polr2l	polymerase (RNA) II (DNA directed) polypeptide L	0.00000422	2.23	NM_025593
Lrig2	leucine-rich repeats and immunoglobulin-like domains 2	0.00000533	3.55	AK158022
Xylt1	xylosyltransferase 1	0.00000637	2.27	NM_175645
Herc1	hect (homologous to the E6-AP (UBE3A) carboxyl terminus) domain and RCC1 (CHC1)-like domain (RLD) 1	0.00000649	2.38	AK035553
Ranbp1	RAN binding protein 1	0.00000698	4.67	AK151167
4930555G01Rik	RIKEN cDNA 4930555G01 gene	0.00000956	2.96	NM_175393
Prickle1	prickle homolog 1 (Drosophila)	0.00001030	2.15	NM_001033217
Down-regulated genes				
Mybph	myosin binding protein H	0.00014600	−2.32	NM_016749
Atrx	alpha thalassemia/mental retardation syndrome X-linked homolog	0.00025200	−2.65	AK172134
Scfd2	sec1 family domain containing 2	0.00079800	−2.02	AK044408
Hyal2	hyaluronidase 2	0.00108229	−3.93	AK087358
Slc35b3	solute carrier family 35, member B3	0.00144001	−2.35	AK167051
Plxdc1	plexin domain containing 1	0.00183679	−2.11	AK040620
Slc17a9	solute carrier family 17, member 9	0.00288047	−2.09	BC019537
Plekhg3	pleckstrin homology domain containing, family G	0.00312320	−2.00	AK080928
Col11a2	collagen, type XI, alpha 2	0.00315107	−2.01	NM_009926
Gkap1	G kinase anchoring protein 1	0.00341408	−2.27	XM_011244543

Supplementary Table 7. The DEGs between the KE and WE groups.

Gene symbol	Gene name	*P* value	Fold change	RefSeq gene name
Up-regulated genes				
Oca2	oculocutaneous albinism II	0.002111519	5.74	NM_021879
Ino80d	INO80 complex subunit D	0.003547891	2.01	AK086434
Rab17	RAB17, member RAS oncogene family	0.004100437	4.23	NM_008998
Slc15a2	solute carrier family 15 (H+/peptide transporter), member 2	0.005312482	3.56	NM_021301
Plekho2	pleckstrin homology domain containing, family O member 2	0.022072747	2.16	AK172714
Tmem192	transmembrane protein 192	0.03725582	2.04	AK090347
Down-regulated genes				
Pibf1	progesterone immunomodulatory binding factor 1	0.004009988	−2.18	AK030385
Gck	glucokinase	0.006009245	−2.56	NM_001287386
Tmco5	transmembrane and coiled-coil domains 5	0.007638294	−2.92	NM_026104
Zkscan7	zinc finger with KRAB and SCAN domains 7	0.009346905	−3.61	NM_001177505
Sp110	Sp110 nuclear body protein	0.009538312	−2.00	NM_175397
Lyve1	lymphatic vessel endothelial hyaluronan receptor 1	0.011785862	−2.01	NM_053247
Ccdc77	coiled-coil domain containing 77	0.013087017	−2.34	NM_026028
Lao1	L-amino acid oxidase 1	0.013674419	−2.23	NM_133892
Popdc3	popeye domain containing 3	0.014859548	−2.36	NM_024286
Pctp	phosphatidylcholine transfer protein	0.015091728	−2.99	BC053478
Bcl11b	B cell leukemia/lymphoma 11B	0.021204049	−2.43	XM_006516114
Gpr150	G protein-coupled receptor 150	0.023718348	−2.17	NM_175495
Egr3	early growth response 3	0.026980145	−2.05	NM_001289925
Zfyve28	zinc finger, FYVE domain containing 28	0.034588687	−2.09	NM_001015039
Lag3	lymphocyte-activation gene 3	0.03522037	−2.04	NM_008479
Tusc3	tumor suppressor candidate 3	0.035297345	−3.98	AK168664
Ccr2	chemokine (C-C motif) receptor 2	0.036493722	−2.17	NM_009915
Hpca	hippocalcin	0.038588762	−2.02	BU504979

Supplementary Table 8. GO terms significantly enriched by Eps8l1 in the comparison of KO versus WT and KE versus KO groups.

ID	GO term	Regulation *P* value (KO VS WT)	Regulation *P* value (KE VS KO)
	Biological Process		
GO:1900029	positive regulation of ruffle assembly	0.003287926	0.009530627
GO:0016601	Rac protein signal transduction	0.009368012	0.026997436
	Cellular Component		
GO:0001726	ruffle	0.034013467	0.004371725
	Molecular Function		
GO:0030676	Rac guanyl-nucleotide exchange factor activity	0.006721637	0.018217986
GO:0042608	T cell receptor binding	0.007678511	0.020794221

Supplementary Table 9. GO terms significantly enriched by Plcb2 between the KO and WT groups.

ID	GO term	Regulation *P* value (KO VS WT)
	Biological Process	
GO:0050913	sensory perception of bitter taste	0.003287926
GO:0001580	detection of chemical stimulus involved in sensory perception of bitter taste	0.014950453
GO:0016042	lipid catabolic process	0.046498252
	Cellular Component	
GO:0005737	cytoplasm	0.047224936
GO:0005829	cytosol	0.489489852
	Molecular Function	
GO:0004629	phospholipase C activity	0.004805373
GO:0004435	phosphatidylinositol phospholipase C activity	0.008634546
GO:0031683	G-protein beta/gamma-subunit complex binding	0.01197408
GO:0008081	phosphoric diester hydrolase activity	0.02240329
GO:0005509	calcium ion binding	0.028870235
GO:0005543	phospholipid binding	0.039253587

Supplementary Table 10. The top 10 enriched GO terms of DEGs between the KO and WT groups.

ID	GO term	Enriched genes	*P* value
	Biological Process		
GO:0050913	sensory perception of bitter taste	Plcb2	0.003287926
GO:1900029	positive regulation of ruffle assembly	Eps8l1	0.003287926
GO:0006975	DNA damage induced protein phosphorylation	Chek1	0.003287926
GO:0048096	chromatin-mediated maintenance of transcription	Chek1	0.004694026
GO:0070257	positive regulation of mucus secretion	Sytl2	0.005162325
GO:0045839	negative regulation of mitotic nuclear division	Chek1	0.005162325
GO:2000279	negative regulation of DNA biosynthetic process	Chek1	0.006566021
GO:0010569	regulation of double-strand break repair via homologous recombination	Chek1	0.007033519
GO:0016601	Rac protein signal transduction	Eps8l1	0.009368012
GO:0031572	G2 DNA damage checkpoint	Chek1	0.009834312
	Cellular Component		
GO:0070382	exocytic vesicle	Sytl2	0.005664978
GO:0005657	replication fork	Chek1	0.009425405
GO:0019897	extrinsic component of plasma membrane	Sytl2	0.012705168
GO:0042470	melanosome	Sytl2	0.012705168
GO:0030863	cortical cytoskeleton	Mpp1	0.015041809
GO:0000794	condensed nuclear chromosome	Chek1	0.019235097
GO:0000781	chromosome, telomeric region	Chek1	0.023875266
GO:0032587	ruffle membrane	Eps8l1	0.02526342
GO:0001726	ruffle	Eps8l1	0.034013467
GO:0005604	basement membrane	Papln	0.04587151
	Molecular Function		
GO:0004629	phospholipase C activity	Plcb2	0.004805373
GO:0042043	neurexin family protein binding	Sytl2	0.006242886
GO:0030676	Rac guanyl-nucleotide exchange factor activity	Eps8l1	0.006721637
GO:0042608	T cell receptor binding	Eps8l1	0.007678511
GO:0004435	phosphatidylinositol phospholipase C activity	Plcb2	0.008634546
GO:0003779	actin binding	Eps8l1;Tns4	0.010618993
GO:0001786	phosphatidylserine binding	Sytl2	0.011497631
GO:0031683	G-protein beta/gamma-subunit complex binding	Plcb2	0.01197408
GO:0008081	phosphoric diester hydrolase activity	Plcb2	0.02240329
GO:0005544	calcium-dependent phospholipid binding	Sytl2	0.02240329

Supplementary Table 11. The top 10 enriched GO terms of DEGs between the KE and KO groups.

ID	GO term	Enriched genes	*P* value
	Biological Process		
GO:0071493	cellular response to UV-B	Hyal2;Cdkn1a	8.09E-05
GO:0006977	DNA damage response	Cdkn1a;Pidd1	0.000118457
GO:0043066	negative regulation of apoptotic process	Mdm4;Bcl11b;Pidd1;Hspa1b;Cdkn1a	0.000407
GO:2001238	positive regulation of extrinsic apoptotic signaling pathway	Hyal2;Pidd1	0.000988155
GO:0055085	transmembrane transport	Itpr2;Oca2;Slc16a8;Kcnq5	0.002144141
GO:0032482	Rab protein signal transduction	Rab17;Rab19	0.003786561
GO:0006886	intracellular protein transport	Rab17;Rab19;Sytl2	0.004540113
GO:0006547	histidine metabolic process	Ftcd	0.008174517
GO:0033153	T cell receptor V(D)J recombination	Bcl11b	0.008174517
GO:0044027	hypermethylation of CpG island	Kcnq1ot1	0.008174517
	Cellular Component		
GO:0042470	melanosome	Rab17;Sytl2	0.000635581
GO:0005622	intracellular	Bcl11b;Hspa1b;Eps8l1;Slfn9; Cdkn1a;Rab17;Ift80	0.001358343
GO:0030139	endocytic vesicle	Hyal2;Rab17	0.002529989
GO:0001726	ruffle	Eps8l1;Frmd4b	0.004371725
GO:0005886	plasma membrane	D930015E06Rik;Hyal2;Veph1;Lima1; Itpr2;Slc16a8;Glra3;Sytl2;Rab17;Rab19	0.010363304
GO:0097458	neuron part	Bcl11b	0.010611343
GO:0000139	Golgi membrane	Hyal2;Ftcd	0.01112583
GO:0000307	cyclin-dependent protein kinase holoenzyme complex	Cdkn1a	0.013247104
GO:0030686	90S preribosome	Gm6252	0.013247104
GO:0070382	exocytic vesicle	Sytl2	0.01587607
	Molecular Function		
GO:0016934	extracellular-glycine-gated chloride channel activity	Glra3	0.007847372
GO:0015129	lactate transmembrane transporter activity	Slc16a8	0.009149467
GO:0051015	actin filament binding	Lima1;Eps8l1	0.010284424
GO:0015278	calcium-release channel activity	Itpr2	0.010449909
GO:0019912	cyclin-dependent protein kinase activating kinase activity	Cdkn1a	0.011748702
GO:0004415	hyaluronon glucosaminidase activity	Hyal2	0.013045847
GO:0008028	monocarboxylic acid transmembrane transporter activity	Slc16a8	0.0156352
GO:0042043	neurexin family protein binding	Sytl2	0.016927413
GO:0004861	cyclin-dependent protein serine/ threonine kinase inhibitor activity	Cdkn1a	0.016927413
GO:0070679	inositol 1,4,5 trisphosphate binding	Itpr2	0.016927413

Supplementary Table 12. The top 10 enriched GO terms of DEGs between the WE and WT groups.

ID	GO term	Enriched genes	*P* value
	Biological Process		
GO:0006900	membrane budding	Trim72;Wasl;Vps4a	0.000156763
GO:0051056	regulation of small GTPase mediated signal transduction	Iqsec3;Rap1gap2;Cdc42bpa	0.0011777
GO:0070588	calcium ion transmembrane transport	Atp2c1;Oprm1;Loxhd1;Cacna1h; Ryr1;Trpm1;Slc8b1	0.001319117
GO:0071320	cellular response to cAMP	Igfbp5;Akap7;Egr3;Hcn1	0.001573349
GO:0015914	phospholipid transport	Pitpnb;Atp11a;Pctp;Tmem30a	0.002442009
GO:2000344	positive regulation of acrosome reaction	Cacna1h;Plb1	0.003180204
GO:0070863	positive regulation of protein exit from endoplasmic reticulum	Slc51b;Tmem30a	0.003180204
GO:0045759	negative regulation of action potential	Cnr2;Hcn1	0.003180204
GO:0018119	peptidyl-cysteine S-nitrosylation	S100a9;S100a8	0.003180204
GO:0009804	coumarin metabolic process	Cyp2a5;Cyp2a4	0.003180204
	Cellular Component		
GO:0042383	sarcolemma	Oprm1;Trim72;Cacna1h;Ryr1; Col6a2;Slc8b1	0.003030434
GO:0016023	cytoplasmic membrane-bounded vesicle	Hyal2;Sgk3;Axin2;Wasl;Chil3	0.0046114
GO:0090543	Flemming body	Vps4a;Ist1	0.005601224
GO:0000139	Golgi membrane	Hyal2;Atp2c1;Xylt1;Wasl;Copg1	0.021606423
GO:0005881	cytoplasmic microtubule	Cyp2a4;Cyp2a5;Axin2	0.030840161
GO:0030992	intraciliary transport particle B	Rabl2;Ttc30a2	0.032204495
GO:0005871	kinesin complex	Kif5b;Kif12;Kif1c	0.033902314
GO:0016607	nuclear speck	Apex1;Dyrk1a;Ppih;1810011O10Rik	0.034440442
GO:0030139	endocytic vesicle	Rabep1;Kif5b;Hyal2	0.03711623
GO:0016529	sarcoplasmic reticulum	Ryr1;Akap7;Syne2	0.038779671
	Molecular Function		
GO:0035662	Toll-like receptor 4 binding	S100a9;S100a8	0.003349627
GO:0016798	hydrolase activity, acting on glycosyl bonds	Hyal2;Lyz1;Lyzl6;Tdg;Chil3	0.004014281
GO:0008536	Ran GTPase binding	Kpnb1;Xpo6;Rangrf	0.005512792
GO:0043425	bHLH transcription factor binding	Usf2;Ep300;Tcf4	0.006090798
GO:0050786	RAGE receptor binding	S100a9;S100a8	0.006996174
GO:0050544	arachidonic acid binding	S100a9;S100a8	0.006996174
GO:0008565	protein transporter activity	Ap2b1;Kpnb1;Xpo6;Rangrf	0.008477855
GO:0003796	lysozyme activity	Lyz1;Lyzl6	0.008478305
GO:0008017	microtubule binding	Kif1c;S100a9;Kif5b;Ppp5c; S100a8;Ska2;Kif12	0.009382088
GO:0019904	protein domain specific binding	Vps4a;E2f4;Oprm1;Ist1;Akap7; Kpnb1;Stx18;Ppp1r2;Tdg	0.011967994

Supplementary Table 13. The top 10 enriched GO terms of DEGs between the KE and WT groups.

ID	GO term	Enriched genes	*P* value
	Biological Process		
GO:0048844	artery morphogenesis	Prrx1;Smad7;Nf1;Stra6;Hes1	0.000102012
GO:0051056	regulation of small GTPase mediated signal transduction	Cdc42bpa;Rap1gap2;Iqsec3	0.002302552
GO:0030325	adrenal gland development	Stra6;Nf1;Pdgfra	0.004916793
GO:0072711	cellular response to hydroxyurea	Rad51;Atrx	0.005029769
GO:0070863	positive regulation of protein exit from endoplasmic reticulum	Tmem30a;Slc51b	0.005029769
GO:0045759	negative regulation of action potential	Cnr2;Hcn1	0.005029769
GO:0065004	protein-DNA complex assembly	Tcf4;Ep300	0.006636052
GO:0006900	membrane budding	Wasl;Vps4a	0.006636052
GO:2000323	negative regulation of glucocorticoid receptor signaling pathway	Phb;Cry1	0.006636052
GO:0017148	negative regulation of translation	Paip2b;Tia1;Gigyf2;Trim71;Igfbp5	0.006900816
	Cellular Component		
GO:0031527	filopodium membrane	Antxr1;Palm;Syne2	0.002901969
GO:0031258	lamellipodium membrane	Antxr1;Syne2	0.006918742
GO:0005793	endoplasmic reticulum-Golgi intermediate compartment	Ptpn2;Rgmb;Nucb1;Ist1	0.008793303
GO:0090543	Flemming body	Vps4a;Ist1	0.008800374
GO:0000139	Golgi membrane	Xylt1;Hyal2;Copg1;Wasl; Arfip1;Atp2c1	0.015973912
GO:0035102	PRC1 complex	Phc2;Cbx8	0.01826734
GO:0000792	heterochromatin	Phc2;Cbx8;Atrx	0.020481389
GO:0005798	Golgi-associated vesicle	Map6d1;Nucb1	0.02108549
GO:0005902	microvillus	Lyz1;Hyal2;Spn;Pdgfra	0.023635841
GO:0016363	nuclear matrix	Zfp326;Scaf8;Runx1t1;Hes1	0.041483935
	Molecular Function		
GO:0015026	coreceptor activity	Gfra4;Rgmb;Cd22	0.003419784
GO:0019904	protein domain specific binding	E2f4;Tdg;Ist1;Kpnb1;Akap7;Scaf8; Ppp1r2;Homer2;Stx18;Vps4a;Spn	0.007541022
GO:0045545	syndecan binding	Sema5a;Nf1	0.008827046
GO:0008022	protein C-terminus binding	Phb;Tcf4;Akap7;Ksr1;Pdzd11; Rad51;Ep300;Vps4a;Hcn1	0.009739438
GO:0008536	Ran GTPase binding	Xpo6;Rangrf;Kpnb1	0.010378605
GO:0043425	bHLH transcription factor binding	Usf2;Tcf4;Ep300	0.011438707
GO:0031490	chromatin DNA binding	Apex1;Prdm14;Vax2;Ep300	0.011540636
GO:0005515	protein binding	Rab3d;Ksr1;Smad7;Gkap1;Ist1;Kcnq 1ot1;Runx1t1;Sim1;Ptpn2;Cbx1;etc	0.013121392
GO:0004629	phospholipase C activity	Plcb2;Plcd4	0.01319896
GO:0032403	protein complex binding	Mb21d2;Casp3;Kpnb1;Ist1;Otof;Pdg fra;Ppfia2;Ins2;Ep300;Apex1;etc	0.014087821

Supplementary Table 14. The top 10 enriched GO terms of DEGs between the KE and WE groups.

ID	GO term	Enriched genes	*P* value
	Biological Process		
GO:0031077	post-embryonic camera-type eye development	Bcl11b	0.007665899
GO:0010574	regulation of vascular endothelial growth factor production	Ccr2	0.007665899
GO:0010837	regulation of keratinocyte proliferation	Bcl11b	0.007665899
GO:0019725	cellular homeostasis	Ccr2	0.007665899
GO:0033153	T cell receptor V(D)J recombination	Bcl11b	0.007665899
GO:0006003	fructose 2,6-bisphosphate metabolic process	Gck	0.007665899
GO:0031584	activation of phospholipase D activity	Hpca	0.008938013
GO:0002829	negative regulation of type 2 immune response	Ccr2	0.008938013
GO:0032811	negative regulation of epinephrine secretion	Gck	0.008938013
GO:0045627	positive regulation of T-helper 1 cell differentiation	Ccr2	0.008938013
	Cellular Component		
GO:0008250	oligosaccharyltransferase complex	Tusc3	0.008992746
GO:0097458	neuron part	Bcl11b	0.010271025
GO:0045180	basal cortex	Gck	0.010271025
GO:0044327	dendritic spine head	Hpca	0.012822804
GO:0005765	lysosomal membrane	Tmem192;Oca2	0.018663317
GO:0032839	dendrite cytoplasm	Hpca	0.028000441
GO:0005768	endosome	Tmem192;Rab17; Zfyve28	0.02954089
GO:0042470	melanosome	Rab17	0.03425766
GO:0032590	dendrite membrane	Hpca	0.03425766
GO:0032809	neuronal cell body membrane	Hpca	0.03425766
	Molecular Function		
GO:0004396	hexokinase activity	Gck	0.007065876
GO:0004340	glucokinase activity	Gck	0.007065876
GO:0005536	glucose binding	Gck	0.01524864
GO:0016493	C-C chemokine receptor activity	Ccr2	0.01757462
GO:0015095	magnesium ion transmembrane transporter activity	Tusc3	0.01757462
GO:0031210	phosphatidylcholine binding	Pctp	0.019895309
GO:0019955	cytokine binding	Ccr2	0.023366447
GO:0005540	hyaluronic acid binding	Lyve1	0.027976222
GO:0004950	chemokine receptor activity	Ccr2	0.029125387
GO:0032266	phosphatidylinositol-3-phosphate binding	Zfyve28	0.03370898

Supplementary Table 15. Common KEGG terms emerged in both comparisons.

ID	KEGG term	Enriched genes (KO VS WT)	Enriched genes (KE VS KO)
Up-regulated pathway			
mmu04115	p53 signaling pathway	Chek1	Cdkn1a, Mdm4, Pidd1
Down-regulated pathway			
mmu04730	Long-term depression	Plcb2	Itpr2
mmu04915	Estrogen signaling pathway	Plcb2	Itpr2, Hspa1b

Supplementary Table 16. The top 20 enriched KEGG terms of DEGs between the KO and WT groups.

ID	KEGG term	Count	PopHit	Enriched	*P* value
mmu05143	African trypanosomiasis	1	36	Plcb2	0.009128992
mmu04973	Carbohydrate digestion and absorption	1	43	Plcb2	0.01085139
mmu04961	Endocrine and other factor-regulated calcium reabsorption	1	54	Plcb2	0.013554988
mmu04730	Long-term depression	1	61	Plcb2	0.015273533
mmu04115	p53 signaling pathway	1	67	Chek1	0.016745379
mmu04720	Long-term potentiation	1	67	Plcb2	0.016745379
mmu04924	Renin secretion	1	72	Plcb2	0.017971077
mmu00562	Inositol phosphate metabolism	1	72	Plcb2	0.017971077
mmu04918	Thyroid hormone synthesis	1	73	Plcb2	0.018216124
mmu04971	Gastric acid secretion	1	74	Plcb2	0.018461142
mmu04970	Salivary secretion	1	78	Plcb2	0.019440905
mmu04911	Insulin secretion	1	85	Plcb2	0.021154313
mmu04540	Gap junction	1	86	Plcb2	0.021398963
mmu04925	Aldosterone synthesis and secretion	1	86	Plcb2	0.021398963
mmu04912	GnRH signaling pathway	1	89	Plcb2	0.02213273
mmu04915	Estrogen signaling pathway	1	96	Plcb2	0.023843784
mmu04713	Circadian entrainment	1	98	Plcb2	0.024332381
mmu04070	Phosphatidylinositol signaling system	1	98	Plcb2	0.024332381
mmu04916	Melanogenesis	1	100	Plcb2	0.024820856
mmu04933	AGE-RAGE signaling pathway in diabetic complications	1	100	Plcb2	0.024820856

Note：Count, the number of genes enriched in specific KEGG terms; PopHit, Population Hit, the number of genes annotated in specific KEGG terms.

Supplementary Table 17. The top 20 enriched KEGG terms of DEGs between the KE and KO groups.

ID	KEGG term	Count	PopHit	Enriched genes	*P* value
mmu04115	p53 signaling pathway	3	67	Cdkn1a;Mdm4;Pidd1	7.11E-05
mmu04210	Apoptosis	3	136	Itpr2;Pidd1;Bcl2a1c	0.000544095
mmu04915	Estrogen signaling pathway	2	96	Itpr2;Hspa1b	0.006126744
mmu04064	NF-kappa B signaling pathway	2	104	Pidd1;Bcl2a1c	0.007135674
mmu04725	Cholinergic synapse	2	113	Itpr2;Kcnq5	0.008355333
mmu04921	Oxytocin signaling pathway	2	153	Cdkn1a;Itpr2	0.014816667
mmu05202	Transcriptional misregulation in cancer	2	177	Cdkn1a;Bcl2a1c	0.019466689
mmu04218	Cellular senescence	2	187	Cdkn1a;Itpr2	0.021566129
mmu00670	One carbon pool by folate	1	19	Ftcd	0.024444178
mmu05167	Kaposi's sarcoma-associated herpesvirus infection	2	204	Cdkn1a;Itpr2	0.025345465
mmu05205	Proteoglycans in cancer	2	206	Cdkn1a;Itpr2	0.025807118
mmu00531	Glycosaminoglycan degradation	1	21	Hyal2	0.02685877
mmu05169	Epstein-Barr virus infection	2	220	Cdkn1a;Hspa1b	0.029136503
mmu00340	Histidine metabolism	1	25	Ftcd	0.031671824
mmu05206	MicroRNAs in cancer	2	281	Cdkn1a;Mdm4	0.045523727
mmu05219	Bladder cancer	1	41	Cdkn1a	0.050710538
mmu05134	Legionellosis	1	58	Hspa1b	0.070569428
mmu04730	Long-term depression	1	61	Itpr2	0.074034863
mmu04213	Longevity regulating pathway-multiple species	1	62	Hspa1b	0.075187421
mmu05214	Glioma	1	64	Cdkn1a	0.077488665

Note：Count, the number of genes enriched in specific KEGG terms; PopHit, Population Hit, the number of genes annotated in specific KEGG terms.

Supplementary Table 18. The top 20 enriched KEGG terms of DEGs between the WE and WT groups.

ID	KEGG term	Count	PopHit	Enriched genes	*P* value
mmu04144	Endocytosis	10	286	Vps4a;Gm8909;Kif5b;Ist1;Iqsec3; H2-Q1;Rabep1;Eea1;Wasl;Ap2b1	0.010638002
mmu03410	Base excision repair	3	35	Apex1;Hmgb1;Tdg	0.017352165
mmu05203	Viral carcinogenesis	8	231	Gm8909;Hist1h2bb;Ep300;Pik3cd ;H2-Q1;Casp3;Ranbp1;Egr3	0.022632799
mmu03013	RNA transport	6	167	Gm9839;AF366264;Kpnb1; Upf3b;Eif3j2;Eif1	0.039646722
mmu00515	Mannose type O-glycan biosynthesis	2	23	Large;B3galnt2	0.050373382
mmu04977	Vitamin digestion and absorption	2	24	Lrat;Plb1	0.054065857
mmu00563	Glycosylphosphatidylinositol (GPI)-anchor biosynthesis	2	25	Pigb;Pigg	0.057851097
mmu04950	Maturity onset diabetes of the young	2	27	Hes1;Ins2	0.065686286
mmu04922	Glucagon signaling pathway	4	102	Phka1;Ep300;Gcgr;Plcb2	0.067782835
mmu05210	Colorectal cancer	3	62	Casp3;Axin2;Pik3cd	0.067995381
mmu04310	Wnt signaling pathway	5	146	Gm9839;Plcb2;Ep300;Axin2; AF366264	0.068196654
mmu05016	Huntington's disease	6	194	Cox7c;Plcb2;Dnal1;Ep300; Casp3;Ap2b1	0.070358373
mmu05146	Amoebiasis	4	106	Plcb2;Casp3;Serpinb6c;Pik3cd	0.075455761
mmu04932	Non-alcoholic fatty liver disease (NAFLD)	5	151	Cox7c;Mlx;Pik3cd;Ins2;Casp3	0.076084982
mmu04931	Insulin resistance	4	109	Mlx;Pik3cd;Ins2;Ppp1r3b	0.081487103
mmu04940	Type I diabetes mellitus	3	70	H2-Q1;Ins2;Gm8909	0.089243539
mmu04520	Adherens junction	3	72	Wasl;Ep300;Pvrl4	0.094944201
mmu05100	Bacterial invasion of epithelial cells	3	76	Elmo1;Wasl;Pik3cd	0.106779222
mmu04960	Aldosterone-regulated sodium reabsorption	2	38	Pik3cd;Ins2	0.114048583
mmu04068	FoxO signaling pathway	4	132	Ins2;Ep300;Pik3cd;Sgk3	0.135038658

Note：Count, the number of genes enriched in specific KEGG terms; PopHit, Population Hit, the number of genes annotated in specific KEGG terms.

Supplementary Table 19. The top 20 enriched KEGG terms of DEGs between the KE and WT groups.

ID	KEGG term	Count	PopHit	Enriched genes	*P* value
mmu04144	Endocytosis	12	286	Eea1;Erbb4;Ist1;Pdgfra;Gm8909; H2-Q1;Kif5b;Rabep1;Ap2b1; Wasl;Vps4a;Iqsec3	0.005018707
mmu00563	Glycosylphosphatidylinositol (GPI)-anchor biosynthesis	3	25	Pigg;Pigb;Pign	0.011800954
mmu00640	Propanoate metabolism	3	31	Pcca;Dbt;Abat	0.020011716
mmu05016	Huntington's disease	8	194	Casp3;Polr2l;Plcb2;Ap2b1;Ep300; Cox7c;Sdha;Dnal1	0.022609904
mmu03410	Base excision repair	3	35	Tdg;Apex1;Hmgb1	0.026853535
mmu04066	HIF-1 signaling pathway	5	105	Pik3cd;Ins2;Ep300;Pgk1;Rps6kb1	0.040315982
mmu04931	Insulin resistance	5	109	Ppp1r3b;Pik3cd;Ins2;Mlx;Rps6kb1	0.045846837
mmu04932	Non-alcoholic fatty liver disease (NAFLD)	6	151	Casp3;Pik3cd;Ins2;Mlx;Cox7c;Sdha	0.052647317
mmu01521	EGFR tyrosine kinase inhibitor resistance	4	80	Pik3cd;Nf1;Rps6kb1;Pdgfra	0.05576429
mmu04630	Jak-STAT signaling pathway	6	159	Pik3cd;Ifna14;Ptpn2;Ep300; Il21r;Il22ra1	0.06394295
mmu04350	TGF-beta signaling pathway	4	85	E2f4;Smad7;Rps6kb1;Ep300	0.066184875
mmu04666	Fc gamma R-mediated phagocytosis	4	87	Wasl;Limk1;Rps6kb1;Pik3cd	0.070618462
mmu05215	Prostate cancer	4	87	Pik3cd;Ins2;Pdgfra;Ep300	0.070618462
mmu05221	Acute myeloid leukemia	3	55	Pik3cd;Runx1t1;Rps6kb1	0.076950579
mmu04621	NOD-like receptor signaling pathway	6	168	Gm5136;Ifna14;Irak4;Plcb2; Naip7;Antxr1	0.078236332
mmu04514	Cell adhesion molecules (CAMs)	6	169	Cd276;Gm8909;H2-Q1;Icosl; Spn;Cd22	0.079927829
mmu00280	Valine, leucine and isoleucine degradation	3	56	Pcca;Dbt;Abat	0.080099124
mmu04068	FoxO signaling pathway	5	132	Pik3cd;Sgk3;Homer2;Ins2;Ep300	0.086039782
mmu04950	Maturity onset diabetes of the young	2	27	Ins2;Hes1	0.087690663
mmu05169	Epstein-Barr virus infection	7	220	Pik3cd;Polr2l;Gm8909;H2-Q1; Ep300;Spn;Adrm1	0.094860112

Note：Count, the number of genes enriched in specific KEGG terms; PopHit, Population Hit, the number of genes annotated in specific KEGG terms.

Supplementary Table 20. The top 20 enriched KEGG terms of DEGs between the KE and WE groups.

ID	KEGG term	Count	PopHit	Enriched genes	*P* value
mmu00524	Neomycin, kanamycin and gentamicin biosynthesis	1	5	Gck	0.003703243
mmu00400	Phenylalanine, tyrosine and tryptophan biosynthesis	1	8	Lao1	0.005550745
mmu00360	Phenylalanine metabolism	1	23	Lao1	0.014747192
mmu04950	Maturity onset diabetes of the young	1	27	Gck	0.01718805
mmu00052	Galactose metabolism	1	32	Gck	0.020232317
mmu00500	Starch and sucrose metabolism	1	33	Gck	0.020840264
mmu00250	Alanine, aspartate and glutamate metabolism	1	37	Lao1	0.023269036
mmu00350	Tyrosine metabolism	1	39	Lao1	0.024481613
mmu00380	Tryptophan metabolism	1	46	Lao1	0.028716153
mmu00270	Cysteine and methionine metabolism	1	48	Lao1	0.029923316
mmu04930	Type II diabetes mellitus	1	48	Gck	0.029923316
mmu00510	N-Glycan biosynthesis	1	49	Tusc3	0.030526448
mmu00520	Amino sugar and nucleotide sugar metabolism	1	49	Gck	0.030526448
mmu01100	Metabolic pathways	3	1316	Gck;Lao1;Tusc3	0.03337417
mmu00280	Valine, leucine and isoleucine degradation	1	56	Lao1	0.034739974
mmu05230	Central carbon metabolism in cancer	1	64	Gck	0.039537479
mmu00010	Glycolysis / Gluconeogenesis	1	66	Gck	0.04073387
mmu04917	Prolactin signaling pathway	1	72	Gck	0.04431589
mmu04911	Insulin secretion	1	85	Gck	0.052040231
mmu04922	Glucagon signaling pathway	1	102	Gck	0.062065844

Note：Count, the number of genes enriched in specific KEGG terms; PopHit, Population Hit, the number of genes annotated in specific KEGG terms.